# Electron-Spin Magnetic Moment (*g* Factor) of $X^2\Sigma^+$ Diatomic Radicals $MX^{(\pm)}$ with Nine Valence Electrons (M = Be, B, Mg, Al; X = N, O, F, P, S, Cl). An ab Initio Study

**Pablo J. Bruna and Friedrich Grein***

*Department of Chemistry, University of New Brunswick, Fredericton, New Brunswick, Canada E3B 6E2*

*Received: September 28, 2000; In Final Form: November 13, 2000*

The electron-spin *g* shifts (magnetic moments $\mu_S$) of $X^2\Sigma^+(1\pi^4 3\sigma)$ radicals $MX^{(\pm)}$ with nine valence electrons are calculated at their equilibrium geometries, using second-order perturbation theory, a Hamiltonian based on Breit−Pauli theory, and correlated (MRCI) wave functions. Eighteen diatomics have been studied: BeF, $BeO^-$, BeCl, MgF, $MgO^-$, and MgCl (class I); $BF^+$, $BCl^+$, $AlF^+$, and $AlCl^+$ (class II); and BO, $BN^-$, BS, $BP^-$, AlO, $AlN^-$, AlS, and $AlP^-$ (class III). Most radicals have small $\Delta g_{\|}$ values ($\approx$−100 ppm) and large negative $\Delta g_\perp$ values (−800 to −8500 ppm), except for $AlN^-$ and $AlP^-$, which have positive $\Delta g_\perp$ values (1400 and 10 000 ppm) due to the quasi-degeneracy $X^2\Sigma^+/1^2\Pi_i$. The sum-over-states expansions for $\Delta g_\perp$ are dominated in classes I and II by the coupling with $1^2\Pi_r$, and in class III with both $1^2\Pi_i$ and $2^2\Pi_r$. The $^2\Pi_r(3\sigma\rightarrow 2\pi)$ state always contributes *negatively*, whereas $^2\Pi_i(1\pi\rightarrow 3\sigma)$ contributes *positively* for most radicals but *negatively* for the boron series BO, $BN^-$, BS, and $BP^-$. Experimental *g* shifts, which are available for eight of the radicals studied here, are generally well reproduced by the $\Delta g$ values calculated at $R_e$. However, for radicals having a very-low-lying $1^2\Pi_i$ state, such as $AlN^-$ and $AlP^-$, our study suggests that future calculations should include vibrational averaging to describe the (unknown) experimental data correctly. Theoretical and experimental $g_\perp$ shifts are compared with those estimated from spin−rotation coupling constants $\gamma$, via Curl's equation.

## Introduction

One of the main purposes of theoretical chemistry is the characterization of the bonding in molecules. One possible way to achieve this objective is to calculate the electric moments of the total charge density distribution, such as dipole and quadrupole moments, for which only the wave function of the electronic state under consideration is required.

Additional information about the bonding in radicals can be obtained from spin-density distributions (either calculated or measured via electron-spin resonance (ESR) spectroscopy), since they are very sensitive to the localization of unpaired electrons.[1−3] The ESR parameters include the hyperfine coupling constants (hfcc's) and electron-spin *g* factors. The isotropic ($A_{iso}$) and dipolar ($A_{dip}$) hfcc's relate to the amount of s and p, d, ... character, respectively, of the open-shell molecular orbital(s). The hfcc's are first-order quantities, like the electric moments.

The *g* factor, which depends on the amount of p, d, ... (non-s) character associated with open-shell MOs, parametrizes the electron-spin magnetic moment $\mu_S = -\mu_B \mathbf{g}\cdot\mathbf{S}$ (where $\mu_B$ is the Bohr magneton, **g** a second rank tensor, and **S** the spin angular-momentum operator). A given $\Delta g$ value ($\Delta g = g - g_e$) describes the change of the *g* factor ($\mu_S$) of a radical relative to that a free electron, with $g_e = 2.002\,319$. In a perturbation theory treatment, $\Delta g$ is evaluated as the sum of first- and second-order contributions.[2] Since the latter include the coupling with excited states, their calculation is not as straightforward as for the hfcc's.

In previous work done in this laboratory, the *g* factors of several radicals $MX^{(\pm)}$ with a $^2\Sigma_{(g,u)}^+$ ground state (GS) have been calculated using perturbation theory, a Hamiltonian based on Breit−Pauli theory, and correlated (MRCI) wave functions, e.g., $H_2^-$,[4] $Li_2^+$, $Li_2^-$, $Be_2^+$,[5] $B_2^+$,[6] $CO^+$,[7] MgF,[8] $C_2^-$, $CSi^-$, $Si_2^-$,[9,10] $F_2^-$, $Cl_2^-$,[11] and $FCl^-$.[12]

A vast series of isoelectronic systems $MX^{(\pm)}$ are those having nine valence electrons (VEs), which constitute the topic of this paper. To facilitate later discussions, these MX systems are divided into sets A−C: in sets A and C, both atoms M and X belong to the first or second row, respectively, while in set B the two atoms are from different rows. Further, each set is subdivided into five classes, from I to V, where class I is the most ionic and class V the most covalent. The radicals investigated are listed in Table 1.

Previous studies[13] have found that *all* $MX^{(\pm)}$ *radicals of sets A and B given in Table 1 have* $X^2\Sigma^+(1\pi^4 3\sigma)$ *ground states* [or $X^2\Sigma_g^+(1\pi_u^4 2\sigma_g)$ for $C_2^-$ and $N_2^+$]. However, the situation for set C is slightly different: the GS of the polar radicals from set C.I to set C.III is also $X^2\Sigma^+$, but for the covalent, or nearly covalent, radicals $SiS^+$,[14] SiP,[15] and $P_2^+$,[13,16] it is $X^2\Pi(1\pi^3 3\sigma^2)$ [or $X^2\Pi_u(1\pi_u^3 2\sigma_g^2)$ for $P_2^+$], whereas $Si_2^-$ has a $X^2\Sigma_g^+(1\pi_u^4 2\sigma_g)$ ground state,[17] like $C_2^-$. Radicals with a $X^2\Pi$ ground state escape ESR detection.[3,18]

For a linear molecule, $\Delta g$ decomposes into one parallel ($\Delta g_{\|}$) and two perpendicular ($\Delta g_\perp$) components. In second-order perturbation theory, $\Delta g$ depends on the spin−orbit (SO) coupling of the GS with particular excited states, as well as on their energetic separation ($\Delta E$) and magnetic dipole transition moment (*L*, the expectation value of the orbital angular-momentum operator), according to the expression $\Delta g \propto (SO)\text{-}L/\Delta E$ for each coupled state.[2,3] The total second-order contribution is given by a sum-over-states (SOS) expansion.

The $\Delta g_{\|}$ component of $X^2\Sigma^+$ radicals, usually very small and varying little between compounds, is determined by first-oder

* To whom correspondence should be addressed. E-mail: fritz@unb.ca.

10.1021/jp003557+ CCC: $20.00 
Published on Web 02/24/2001

**TABLE 1: Selected List of $X^2\Sigma_{(g)}^+$ Radicals $MX^{(\pm)}$ with Nine Valence Electrons (M and X from the First and Second Rows)[a]**

| class[b] | set A | set B | set C |
|---|---|---|---|
| I | BeF, $BeO^-$ | BeCl, MgF, $MgO^-$ | MgCl |
| II | $BF^+$ | $BCl^+$, $AlF^+$ | $AlCl^+$ |
| III | BO, $BN^-$ | BS, AlO, $BP^-$, $AlN^-$ | AlS, $AlP^-$ |
| IV | $CO^+$, CN | $CS^+$, $SiO^+$, CP, SiN | $SiS^+$, SiP |
| V | $C_2^-$, $N_2^+$ | $CSi^-$, $NP^+$ | $Si_2^-$, $P_2^+$ |

[a] CaF was studied in ref 20. [b] Classes I−III are investigated in this work, while classes IV and V are discussed in ref 19.

contributions; i.e., the coupling with excited states is weak.[3] Because of their relatively low physical content, $\Delta g_{\|}$ values will not be analyzed in detail.

On the other hand, $\Delta g_\perp$ depends on the coupling with the $^2\Pi$ manifold, therefore giving valuable insight into the structure of such excited states. For $X^2\Sigma^+(2\sigma^2 1\pi^4 3\sigma)$ radicals, as will be shown later, the SOS expansions for $\Delta g_\perp$ depend mostly on the coupling with $^2\Pi_i(2\sigma^2 1\pi^3 3\sigma^2)$, the *inverted* $^2\Pi$ state generated by the excitation $1\pi \rightarrow 3\sigma$, and $^2\Pi_r(2\sigma^2 1\pi^4 2\pi)$, the *regular* $^2\Pi$ state generated by the excitation $3\sigma \rightarrow 2\pi$.

In the above, $3\sigma$ is the GS singly occupied MO (SOMO), and $2\pi$ the $\pi^*$ LUMO of valence character. Hereafter, $^2\Pi_i$-$(1\pi^3 3\sigma^2)$ and $^2\Pi_r(1\pi^4 2\pi)$ will be abbreviated as $^2\Pi_i(1\pi)$ and $^2\Pi_r(2\pi)$, respectively; please, also note that in this work only VEs are numbered.

The variation of $\Delta g_\perp$ among MX radicals partly depends on the changes in the spin-density distribution taking place between $X^2\Sigma^+$ and $^2\Pi_i$, $^2\Pi_r$–with such density being generally localized on M, X, and M, respectively. In addition, when passing from class I to class V, the energy ordering of the $^2\Pi$ states r and i changes from r < i to r ≈ i to i < r. As well, between sets A and C, $\Delta E$ generally decreases and $\langle X^2\Sigma^+|SO|^2\Pi\rangle$ increases, both changes favoring larger $g_\perp$ shifts for heavier diatomics.

In short, the second-order coupling $X^2\Sigma^+/n^2\Pi$ ($n = 1, 2, ...$) should vary markedly among sets and classes, and in fact, plenty of ESR $g$ data for nine-VE radicals prove our statement.[3] Evidently, a comparative analysis of the experimental data appears to be very difficult without having detailed information on the parameters governing $g$ factors. Although $\Delta E$ values are often available from optical spectroscopy, practically nothing is known about off-diagonal $L$ and SO values. A theoretical study thus appears to be of help in rationalizing experimental $g$ factors.

An additional goal—besides the calculation of $g$ shifts per se—is to relate the changes in bonding to $\mu_S$. While the connection between hfcc's and bonding has been reported for several of these MX systems, very little work has been done on their magnetic moments.[3]

In this paper, we focus on $MX^{(\pm)}$ radicals from classes I−III, all having pronounced ionic bonding. Radicals of more covalent character (IV and V) will be discussed separately.[19] In a preliminary account,[20] the $g$ shifts calculated for BO, AlO, $CO^+$, $SiO^+$, and MF (M = Be, Mg, Ca) were compared with those of other first- and second-row systems ($O_2^-$, $S_2^-$, $F_2^-$, $Cl_2^-$, and $FCl^-$).

## Methods

The AO basis sets used are 6-311+G(2d) for first-row atoms[21a] and McLean−Chandler for those of the second row,[21b] as provided in Gaussian90.[22] The GS SCF MOs were used for the uncorrelated (GSTEPS)[23,24] calculations. The GS natural orbitals (NOs) were employed for the correlated $g$ shifts, using a multireference configuration interaction (MRCI) method.[25]

The frozen-core approximation has been used; i.e., there are no excitations from core MOs ($1s^2$ and $1s^2 2s^2 2p^6$ for first- and second-row atoms, respectively) and the complementary virtual orbitals are discarded. In the first step, nine $^2\Pi$ states were calculated simultaneously, and thereafter more refined calculations were done by selecting one or two $^2\Pi$ states only. In the latter, the use of a smaller selection threshold allowed for better wave functions.

Details about the theoretical study of electron-spin $g$ factors, using perturbation theory up to second order and a Hamiltonian based on Breit−Pauli theory,[2] are given in previous papers.[7,23,24] In short, each $\Delta g$ component is given by the sum of (1) a first-order term, evaluated as an expectation value over the GS wave function (presently at the uncorrelated ROHF level), and (2) a second-order term, or SOS expansion, requiring the evaluation of $\Delta E$, and off-diagonal SO and $L$ matrix elements (between $X^2\Sigma^+$ and low-lying $^2\Pi$ states in the case of $\Delta g_\perp$). This term is calculated with MRCI wave functions.

In second order, the $\Delta g_{\|}$ component of a $X^2\Sigma^+$ radical depends on the magnetic coupling with $^2\Sigma^-$ states. MRCI calculations on $CO^+$ [7] and MgF[8] have shown that these contributions to $\Delta g_{\|}$ are practically zero. For this reason, they are not included here.

The theoretical $g$ shifts are calculated at $R_e$, the GS equilibrium geometry (experimental values if known,[13] MRDCI values for $BN^-$ [26] and $AlP^-$,[27] and results from MP2/6-311+G(2df) optimizations[22] for $BP^-$ and $AlN^-$, this work). The electronic charge centroid,[28] calculated at the ROHF level, is taken as the origin of coordinates.

## General Trends for $\Delta E$, $L$, and SO Parameters

We discuss below general trends for the quantities determining the second-order contribution to $\Delta g_\perp$(MX): the vertical $\Delta E(^2\Pi)$ and the matrix elements $\langle X^2\Sigma^+(3\sigma)|L|^2\Pi\rangle$ and $\langle X^2\Sigma^+$-$(3\sigma)|SO|^2\Pi\rangle$, with $^2\Pi$ standing for $^2\Pi_i(1\pi)$ or $^2\Pi_r(2\pi)$.

**Vertical Excitation Energies.** Table 2 compares the vertical $\Delta E$ values of $^2\Pi_i$ and $^2\Pi_r$, as calculated at the MRCI level, with experimental and theoretical $T_e$ values from the literature. The GS bond distances ($R_e$) are also specified.

Our $\Delta E$ values reproduce the $T_e$ data very well, particularly if one notes that vertical $\Delta E$ values have to be slightly larger than the corresponding adiabatic values.

No theoretical work had been done on the excited states of $BCl^+$. A CCSD(T) study reported some GS data ($R_e$, $\omega_e$, and IP(BCl)).[29] We place the $1,2^2\Pi$ states at 4.45 and 5.32 eV (vertical). In contrast with other $MX^+$ ions, the two $^2\Pi$ states of $AlCl^+$ are relatively well separated: in the vertical region, according to ref 30, $1^2\Pi_i$ and $2^2\Pi_r$ lie at 2.95 and 4.65 eV, respectivley. These values are well reproduced here.

Among class III radicals, the current knowledge on $BN^-$ and $AlP^-$ is based solely on ab initio results;[26,27] nothing has been reported for $AlN^-$ and $BP^-$. Further, an SCF/CI study on BS reported a $T_e(1^2\Pi_i)$ of 3.83 eV,[31] largely overestimating experimental results, but $T_e(2^2\Pi_r)$ was better described (Table 2).

The $1^2\Pi_i$ state of AlO has $T_e = 0.67$ eV, much smaller than $T_e \approx 2$ eV for BS (a set B radical like AlO) but similar to 0.57 eV reported for AlS (set C). These data indicate that AlO has an anomalously small $\Delta E(1^2\Pi_i)$.

When comparing radicals within a given set, it is seen that $\Delta E(1^2\Pi)$ generally increases along the classes III < I < II. In

**TABLE 2: Ground-State $R_e$ Values and Excitation Energies (eV) for the Lowest-Lying $^2\Pi$ States[a]**

| radical (set, class) | $R_e(X^2\Sigma^+)$ (bohr) | $1^2\Pi$ | | $2^2\Pi$ | |
|---|---|---|---|---|---|
| | | $\Delta E$ | $T_e$[b] | $\Delta E$ | $T_e$[b] |
| BeF (A, I) | 2.572 | 4.35 | 4.12 | 7.90 | (7.8) [T34] |
| $BeO^-$ | 2.579 | 2.37 | | 3.54 | |
| BeCl (B, I) | 3.396 | 3.61 | 3.47 | 5.75 | |
| MgF | 3.310 | 3.59 | 3.45 | 6.28 ($3^2\Pi$) | |
| $MgO^-$ | 3.390 | 0.70 | | 2.47 | |
| MgCl (C, I) | 4.156 | 3.33 | 3.29 | 4.56 | (4.4) [T67] |
| $BF^+$ (A, II) | 2.336 | 6.48 | | 7.85 | (7.6) [T68] |
| $BCl^+$ (B, II) | 3.018 | 4.45 | | 5.32 | |
| $AlF^+$ | 3.022 | 5.26 | (5.21) [T30] | 5.65 | (5.5) [T30,T32] |
| $AlCl^+$ (C, II) | 3.849 | 2.93 | (2.95) [T30] | 4.67 | (4.65) [T30,T33] |
| BO (A, III) | 2.276 | 3.53 | 2.97 | 7.39 | 6.86 |
| $BN^-$ | 2.440 | 0.88 | 0.78 [T26] | 5.98 | |
| BS (B, III) | 3.041 | 2.47 | 1.99 | 5.07 | 4.83 |
| $BP^-$ | 3.140 | 1.19 | | 4.16 | |
| AlO | 3.057 | 0.99 | 0.67 | 4.22 | 4.11 |
| $AlN^-$ | 3.132 | 0.32 | | 3.15 | |
| AlS (C, III) | 3.834 | 0.89 | 0.57 [60] | 3.85 | 3.73 |
| $AlP^-$ | 4.089 | 0.18 | 0.08 [T27][c] | 3.02 | 2.13 [T27][c] |

[a] $\Delta E$, vertical (this work, MRCI data); $T_e$, adiabatic. [b] Experimental data.[13] Vertical $\Delta E$ given in parentheses, and theoretical studies as [T*xx*]. [c] $\Delta E(1^2\Pi) = 0.23$ eV, and $\Delta E(2^2\Pi) = 2.89$ eV.

set A, for example, $\Delta E(1^2\Pi)$ of BO, BeF, and $BF^+$ is ca. 3.5, 4.3, and 6.5 eV, respectively. The same holds for BS, BeCl, and $BCl^+$ of set B, with $\Delta E$ values increasing from 2.5 to 4.4 eV. As expected, $\Delta E(1^2\Pi)$ decreases from set A to set C.

It is worth noting that $\Delta E(1^2\Pi)$ values below 1 eV for $BN^-$, $MgO^-$, AlO, and AlS—and particularly for $AlN^-$ and $AlP^-$, with $\Delta E \leq 0.3$ eV—are significantly smaller than for all other radicals, a feature which should be kept in mind for later comparisons of $\Delta g_\perp$ values. Also, $\Delta E(1^2\Pi)$ increases approximately by a factor of 2 between BO and $BF^+$, but decreases by a factor of 4 between BO and $BN^-$. This illustrates, from an energetic point of view, how sensitive the *g* factor could be to replacing O by the isovalent ion $F^+$ or $N^-$.

As seen in Table 2, the $\Delta E$ values for $2^2\Pi$ are more uniform within each class, and are reproduced fairly well by averages of 7.7, 5.3, and 4.6 eV for sets A−C, respectively.

The actual picture is more complicated than sketched above since the ordering of the $^2\Pi_r$ and $^2\Pi_i$ states is not the same for all classes. According to the literature,[13] the $1^2\Pi$ state corresponds to $^2\Pi_r(2\pi)$ in class I, to $^2\Pi_i(1\pi)$ in class III, and to either one in class II, depending on the radical.[30,32,33] Complementarily, $2^2\Pi$ correlates with $^2\Pi_i(1\pi)$ in class I, but with $^2\Pi_r(2\pi)$ in class III. (In class I radicals, $2^2\Pi$ is actually of Rydberg character, while the valence $^2\Pi$ state occupying $2\pi(\pi^*)$ lies somewhat higher. See, for example, the study on BeF by Marian.[34] Rydberg states, however, do not contribute to the *g* factor.[8,35]).

One should also note that $^2\Pi_r(2\pi)$ is a *bound* state for all radicals from classes I−III, whereas $^2\Pi_i(1\pi)$ is *repulsive* in classes I and II but *bound* in class III. (These features might be of relevance when vibrational averaging is included in the *g* factor calculations.)

***L Parameters.*** The magnetic coupling of $X^2\Sigma^+(1\pi^4 3\sigma)$ with $^2\Pi_i(1\pi^3 3\sigma^2)$ and $^2\Pi_r(1\pi^4 2\pi)$ is ultimately determined by the compositions of $3\sigma$, $1\pi$, and $2\pi$. These MOs correlate, respectively, with $2\sigma_g(p_\sigma+p_\sigma$ plus some s+s), $1\pi_u(p_\pi+p_\pi)$, and $1\pi_g(p_\pi-p_\pi)$, of homonuclear $M_2$. (In $D_{\infty h}$ symmetry, $\sigma_g$ couples magnetically only with $\pi_g$.) For heteronuclear MX, the $3\sigma$, $1\pi$, and $2\pi$ MOs are described by less symmetrical linear combinations, namely

$$3\sigma = a_1 s + a_2 p_\sigma - a'_3 s' - a'_4 p'_\sigma$$

with unprimed and primed labels corresponding to centers M

$$1\pi = b_1 p_\pi + b'_2 p'_\pi$$

$$2\pi = c_1 p_\pi - c'_2 p'_\pi$$

and X, respectively. For bond distances close to $R_e(X^2\Sigma^+)$, both $3\sigma$ and $2\pi$ are largely localized on the less electronegative atom M (Be, B, Mg, Al), with the $3\sigma$ SOMO consisting mostly of an $sp_\sigma$ lone pair and $2\pi$ corresponding to $p_\pi(M)$. Complementarily, $1\pi$ is mainly composed of $p_\pi$ AOs on the more electronegative atom X (N, O, F, P, S, Cl).

The localization of the electron density is almost complete for the strongly polar classes I and II, where a given MO is mainly described by M *or* X AOs. Very little charge density is found along the bond. On the other hand, in class III the valence MOs are *polarized* toward either M or X, but the net charge transfer M → X is not as extreme as for classes I and II. In fact, in class III radicals there is a substantial charge density within the bonding region, due to covalent contributions. Because of this more balanced charge delocalization in III—particularly for $1\pi$ showing bonding characteristics close to those of $1\pi_u$–the excited state $^2\Pi_i(1\pi)$ has a bound potential. This behavior contrasts with its repulsive character in classes I and II.

The $\langle X^2\Sigma^+|L|^2\Pi\rangle$ parameter relates the $X^2\Sigma^+$ spin-density distribution to that of the $^2\Pi$ state ($^2\Pi_i$ or $^2\Pi_r$). It is large when both lower and upper states have equivalent spin-density distributions, i.e., when rotating the wave function $\Psi(X^2\Sigma^+)$ about an axis perpendicular to the M−X bond leads to an optimal overlap with $\Psi(^2\Pi)$. Considering the relative stabilities of the two $^2\Pi$ states and the MO compositions discussed earlier, *L* should be generally large for the coupling of $X^2\Sigma^+(3\sigma)$ with $^2\Pi_r(2\pi)$, i.e., $1^2\Pi$ in class I and $2^2\Pi$ in class III, but much smaller for the coupling with $^2\Pi_i(1\pi)$.

**SO Parameters.** To rationalize the SO data, it is useful to relate $\langle X^2\Sigma^+(3\sigma)|SO|^2\Pi\rangle$ to matrix elements involving AOs. At the monodeterminantal level, $\langle X^2\Sigma^+(3\sigma)|SO|^2\Pi_i(1\pi)\rangle$ is represented by the matrix element $\langle 3\sigma|SO|1\pi\rangle$, which in terms of

**TABLE 3: MRCI Values of $\Delta E$ (eV), SO ($cm^{-1}$), $L$ (au), and $\Delta g$ (ppm) for the $X^2\Sigma^+$ State of MF, MCl, and $MO^-$ Radicals (M = Be, Mg) of Class I[a]**

| $g$ shift | BeF | BeO[b] | BeCl | MgF | MgO[b] | MgCl |
|---|---|---|---|---|---|---|
| $\Delta g_{\|\|}$(tot) | −50 | −36 | −55 | −54 | −49 | −61 |
| $\Delta g_\perp$ | | | | | | |
| $1^2\Pi_r(2\pi)$ | | | | | | |
| $\Delta E$ | 4.345 | 2.372 | 3.607 | 3.585 | 0.695 | 3.330 |
| SO | −6.785 | 10.894 | 20.438 | 13.683 | 19.939 | 25.532 |
| $L$ | 0.905 | −0.288 | −1.126 | −0.796 | 0.009 | −1.096 |
| $\Delta g$ | −720 | −657 | −3249 | −1548 | 122 | −4278 |
| $2^2\Pi_i(1\pi)$ | | | | | | |
| $\Delta E$ | 7.900 | 3.542 | 5.749 | 6.280[c] | 2.467 | 4.558 |
| SO | 6.390 | −3.021 | 48.206 | −12.124 | −12.723 | −53.339 |
| L | −0.080 | 0.641 | 0.089 | 0.150 | 0.830 | −0.066 |
| $\Delta g$ | −33 | −271 | 381 | −147 | −2124 | 392 |
| $(3-9)^2\Pi$ | | | | | | |
| $\Sigma\Delta g$ | −31 | −552 | −238 | −94[d] | −492 | −385 |
| $\Sigma$(2nd) | −784 | −1480 | −3106 | −1789 | −2494 | −4271 |
| 1st | −39 | −24 | −22 | −20 | −17 | 7 |
| $\Delta g_\perp$(tot) | −823 | −1504 | −3128 | −1809 | −2511 | −4264 |
| $\langle\Delta g\rangle$[e] | −565 | −1015 | −2104 | −1224 | −1690 | −2863 |

[a] See ref 20 for CaF. [b] $^2\Pi_r(2\pi)$ corresponds to the $2^2\Pi$ state. [c] $3^2\Pi$. [d] $(2,4-9)^2\Pi$. [e] Isotropic shift $\langle\Delta g\rangle = (\Delta g_{\|} + 2\Delta g_\perp)/3$.

AOs becomes

$$\langle 3\sigma|\mathrm{SO}|1\pi\rangle = b_1\{a_1\langle \mathrm{s}||\mathrm{p}_\pi\rangle + a_2\langle \mathrm{p}_\sigma||\mathrm{p}_\pi\rangle - a'_3\langle \mathrm{s}'||\mathrm{p}_\pi\rangle - a'_4\langle \mathrm{p}'_\sigma||\mathrm{p}_\pi\rangle\} + b'_2\{a_1\langle \mathrm{s}||\mathrm{p}'_\pi\rangle + a_2\langle \mathrm{p}_\sigma||\mathrm{p}'_\pi\rangle - a'_3\langle \mathrm{s}'||\mathrm{p}'_\pi\rangle - a'_4\langle \mathrm{p}'_\sigma||\mathrm{p}'_\pi\rangle\}$$

where || stands for |SO|. Under the conditions that $\langle \mathrm{s}|\mathrm{SO}|\mathrm{p}_{\sigma,\pi}\rangle = 0$, and matrix elements involving two different atomic centers are negligible, it follows that

$$\langle X^2\Sigma^+(3\sigma)|\mathrm{SO}|^2\Pi_i(1\pi)\rangle \approx a_2b_1\langle \mathrm{p}_\sigma|\mathrm{SO}|\mathrm{p}_\pi\rangle_M - a'_4b'_2\langle \mathrm{p}'_\sigma|\mathrm{SO}|\mathrm{p}'_\pi\rangle_X \quad (1)$$

Similarly, the coupling with $^2\Pi_r(2\pi)$ can be approximated as

$$\langle X^2\Sigma^+(3\sigma)|\mathrm{SO}|^2\Pi_r(2\pi)\rangle \approx a_2c_1\langle \mathrm{p}_\sigma|\mathrm{SO}|\mathrm{p}_\pi\rangle_M + a'_4c'_2\langle \mathrm{p}'_\sigma|\mathrm{SO}|\mathrm{p}'_\pi\rangle_X \quad (2)$$

According to eqs 1 and 2, $\langle X^2\Sigma^+(3\sigma)|\mathrm{SO}|^2\Pi\rangle$ simply corresponds to the linear combination of matrix elements involving the $p_\sigma$ and $p_\pi$ AOs at each center. Further, the relative weight of center M in $\langle 3\sigma|\mathrm{SO}|1\pi\rangle$ is given by the product of $a_2$ and $b_1$–the amount of $p_\sigma$(M) and $p_\pi$(M) character in $3\sigma$ and $2\pi$, respectively—while that of center X is given by the equivalent product $a'_4b'_2$.

If there were no $p_\sigma$(X) contribution to $3\sigma$ (i.e., $a'_4 = 0$), the $\langle 3\sigma|\mathrm{SO}|1\pi\rangle$ value would be given by $a_2b_1\langle \mathrm{p}_\sigma|\mathrm{SO}|\mathrm{p}_\pi\rangle_M$. Assuming that $\langle \mathrm{p}_\sigma|\mathrm{SO}|\mathrm{p}_\pi\rangle_M$ is proportional to $\lambda$(M), the spin−orbit constant of atom M, $\langle 3\sigma|\mathrm{SO}|1\pi\rangle$ should be approximately $a_2b_1\lambda$(M). Similarly, $\langle 3\sigma|\mathrm{SO}|2\pi\rangle$ would correspond to $a_2c_1\lambda$(M).

According to the above approximations, the SO matrix elements between $X^2\Sigma^+(3\sigma)$ and the $^2\Pi_i(1\pi)$ and $^2\Pi_r(2\pi)$ states are expected to lie close to the atomic $\lambda$(M) values. For the M atoms Be, B, Mg, Al, etc., $\lambda$ is positive and small, ranging from about 2 $cm^{-1}$ for Be to 75 $cm^{-1}$ for Al. On the other hand, the $\lambda$(X) values of F and Cl are negative and much larger, −269 and −587 $cm^{-1}$, respectively.[36,37]

As shown later, both SO values are generally somewhat larger than $\lambda$(M), an indication that $3\sigma$ has s and $p_\sigma$ contribution from M *and* X.

### Results for $g$ Shifts

The $g$ shifts calculated for classes I−III radicals are summarized in Tables 3−5, respectively.

**Class I: BeF, BeCl, MgF, MgCl, $BeO^-$, and $MgO^-$.** As seen in Table 3, the total $\Delta g_\perp$ values are governed by the coupling with $^2\Pi_r$, which contributes negatively. Such predominance relates to the large $|L|$ values (∼1 au), as $3\sigma$ and $2\pi$ are both mainly localized on M. The $2^2\Pi_i(1\pi)$ state contributes little because $1\pi$ is mostly $p_\pi$(X), resulting in small $|L|$ (∼0.1 au).

Previous studies have found that the s(M) character of $3\sigma$ increases from 48% in BeF to 60% in BaF, while the p(M) contribution, or $sp_\sigma$(M) hybridization, complementarily decreases along this series.[3,38] As well, for the fluorides and chlorides BeX and MgX, the spin density is large for Be and Mg (∼0.975), and small *but not zero* (∼0.025) for F and Cl.[38−40]

Thus, at equilibrium these radicals mainly have an ionic composition $M^+(3\sigma)X^-(2\sigma^21\pi^4)$, with some admixture of the covalent structure $M(3\sigma^2)X(2\sigma1\pi^4)$. Each open-shell $\sigma$ MO has s and $p_\sigma$ contributions, with s(M) dominating in $3\sigma$ and $p_\sigma$(X) in $2\sigma$.

The $\Delta g$ values of $Be^+$ and $Mg^+$, which only depend on first-order contributions, are isotropic and small (−55 ± 5 ppm). First-order contributions to $\Delta g_{\|}$ and $\Delta g_\perp$ of MX are also small (−20 to −60 ppm), practically retaining the atomic values. However, second-order contributions to $\Delta g_\perp$ are large (−800 to −4300 ppm), providing some measure of the $p_\sigma$ contributions to $3\sigma$.

Substitution of F by Cl results in an increase of $|\Delta g_\perp|$ by a factor of 3.7 for BeF/BeCl and of 2.3 for MgF/MgCl. The principal reason for such an increase of $|\Delta g_\perp|$ is $\langle X^2\Sigma^+|\mathrm{SO}|1^2\Pi_r\rangle$, which according to Table 3 increases approximately by a similar factor of 3 between BeF and BeCl (∼6.8 vs 20.4 $cm^{-1}$) and of 2 between MgF and MgCl (∼13.7 vs 25.5 $cm^{-1}$). This matrix element, which is essentially $\langle 3\sigma|\mathrm{SO}|2\pi\rangle$, would have remained almost the same between BeF and BeCl—or between MgF and MgCl—if p AOs only on M were contributing to $3\sigma$ and $2\pi$. Since this is not the case, p AOs on X also contribute.

According to the atomic data,[36,37] the ratio $\lambda(F)/\lambda(M^+)$ is very large for $Be^+$ (∼300), but significantly smaller for $Mg^+$ (∼3). Replacing F by Cl, these ratios practically double. Thus, a small admixture of p(F,Cl) into $3\sigma$ and $2\pi$ results in much larger SO values than expected if both MOs had been localized on M only, which in turn is reflected in the higher $g_\perp$ shifts. This effect is obviously more important for BeX than MgX systems.

Metal substitution Be → Mg → Ca also causes an increase in $|\Delta g_\perp|$, but on a smaller scale than halogen replacement, by

**TABLE 4: MRCI Values of $\Delta E$ (eV), SO ($cm^{-1}$), $L$ (au), and $\Delta g$ (ppm) for the $X^2\Sigma^+$ State of $MF^+$ and $MCl^+$ Radicals (M = B, Al) of Class II**

| $g$ shift | $BF^+$ | $BCl^+$ | $AlF^+$ | $AlCl^+$ |
|---|---|---|---|---|
| $\Delta g_{\|\|}$(tot) | −108 | −117 | −109 | −118 |
| $\Delta g_\perp$ | | | | |
| $1^2\Pi^a$ | | | | |
| $\Delta E$ | 6.477 | 4.447 | 5.256 | 2.930 |
| SO | −24.954 | −79.387 | 46.726 | 88.040 |
| $L$ | 0.942 | 0.635 | −0.812 | −0.061 |
| $\Delta g$ | −1848 | −5778 | −3676 | −932 |
| $2^2\Pi^b$ | | | | |
| $\Delta E$ | 7.850 | 5.323 | 5.649 | 4.673 |
| SO | −23.352 | 3.798 | 12.326 | 43.466 |
| $L$ | −0.261 | 0.995 | 0.367 | −1.206 |
| $\Delta g$ | 395 | 362 | 407 | −5713 |
| $(3-9)^2\Pi$ | | | | |
| $\Sigma\Delta g$ | −111 | −157 | 54 | 58 |
| Σ(2nd) | −1564 | −5573 | −3215 | −6587 |
| 1st | −69 | −47 | −49 | −3 |
| $\Delta g_\perp$(tot) | −1633 | −5620 | −3264 | −5490 |
| $\langle\Delta g\rangle$ | −1125 | −3786 | −2212 | −4433 |

[a] $^2\Pi_r(2\pi)$ for $MF^+$ and $^2\Pi_i(1\pi)$ for $MCl^+$. [b] $^2\Pi_i(1\pi)$ for $MF^+$ and $^2\Pi_r(2\pi)$ for $MCl^+$.

a factor of about 2.2 for BeF/MgF, 1.6 for MgF/CaF, and 1.4 for BeCl/MgCl.

The $\Delta E$ values for $BeO^-$ and $MgO^-$, both anions being stable upon electron detachment,[41] are smaller than for BeF and MgF, respectively, resulting in total $\Delta g_\perp$ values about −700 ppm lower than those for the fluorides (Table 3).

In summary, the SO values calculated for the coupling $X^2\Sigma^+$-$(3\sigma)/1^2\Pi_r(2\pi)$ in class I radicals—which are larger than the atomic $\lambda$(M) values—indicate that $3\sigma$ has $sp_\sigma$ contributions *from both centers M and X*, as already known via the hfcc's.[38−40]

There is only one theoretical study allowing for comparisons. For the Λ doubling of BeF, Cooper et al.[42] reported for $1^2\Pi_r$ absolute values of 6.01 $cm^{-1}$ for SO and of 1.28 au for $L_+$ (at $R = 2.6$ bohr, close to $R_e$, Table 2). Our MRCI results are similar to theirs (−6.79 $cm^{-1}$ and 0.91 au, Table 3). Note that $|L| = (2)^{-1/2}L_+$.

**Class II: $BF^+$, $BCl^+$, $AlF^+$, and $AlCl^+$.** According to Table 4, the $\Delta g_{\|\|}$ values of $MX^+$ cations lie near −110 ppm. They are essentially the same as for $B^{2+}$ and $Al^{2+}$, both being ≈−105 ppm (about twice the values for $Be^+$ and $Mg^+$, reflecting the larger $Z_{eff}$ in $M^{2+}$). This simple comparison corroborates previous studies[30,32] indicating that $X^2\Sigma^+$ near $R_e$ is mainly described by the ionic structure $M^{2+}(3\sigma)X^-(1\pi^4)$, equivalent to that prevailing in class I.

However, since the lowest dissociation limit of $MX^+$ is $M^+$-$(s^2)$ + $X(p^5)$, the structure $M^+(\sigma^2)X(\sigma\pi^4)$ may also contribute to the bonding. Due to the $\sigma$ open shell in X, mostly $p_\sigma$(X), this structure should enhance the SO values of $MX^+$, as for MX radicals from class I.

The largest contribution to $\Delta g_\perp(MX^+)$ arises from the coupling with $1^2\Pi$, except for $AlCl^+$, where $2^2\Pi$ dominates. In all cases, such coupling involves $^2\Pi_r(2\pi)$. This feature confirms expectations (see above), and is in line with what is known from the literature.[3]

According to experimental[33] and theoretical studies,[30,32] the relative stabilities of the $^2\Pi_i(1\pi)$ and $^2\Pi_r(2\pi)$ states depend on the identity of $MX^+$: in passing from set A to set C, $^2\Pi_i$ becomes gradually more stable than $^2\Pi_r$; e.g., the ordering is $1^2\Pi_r < 2^2\Pi_i$ for $BF^+$ but $1^2\Pi_i < 2^2\Pi_r$ for $AlCl^+$ (the only $MX^+$ radical with a discrete band in the spectrum).[33] Also, in class II the energy separation between $^2\Pi_r$(bound) and $^2\Pi_i$(repulsive) is generally small (and smaller than for class I, Table 2). The strong mixing of bound and repulsive potentials in $BF^+$, $BCl^+$, and $AlF^+$ explains the absence of structured bands in their chemiluminiscence spectra.[33]

The strong interaction between $^2\Pi_r(3\sigma\rightarrow2\pi)$ and $^2\Pi_i(1\pi\rightarrow3\sigma)$ implies that both states should contribute to $\Delta g_\perp(MX^+)$ (in contrast to class I radicals, where this mixing is very weak in the Franck−Condon region). Such interaction is reflected in the mixed $L$ values calculated for the two $^2\Pi$ states of $BF^+$, $AlF^+$, and $BCl^+$ (Table 4). For $AlCl^+$, the situation is clear: a large $|L| \approx 1.2$ au for $2^2\Pi$ reveals an unperturbed $^2\Pi_r(3\sigma\rightarrow2\pi)$ composition.

A total $\Delta g_\perp = -1633$ ppm calculated for $BF^+$ is dominated by the $1^2\Pi$ contribution (−1848 ppm). The same holds for $\Delta g_\perp$ of $AlF^+$ (−3676 vs −3264 ppm) and $BCl^+$ (−5778 vs −5620 ppm). The $2^2\Pi$ coupling is small, positive, and around 400 ppm (Table 4).

In contrast, a $\Delta g_\perp$(tot) of −6590 ppm for $AlCl^+$ is dominated by $2^2\Pi$ ($2^2\Pi_r$). The $1^2\Pi_i$ state, despite its small magnetic overlap ($L = -0.061$ au), contributes to the total $\Delta g_\perp$ about 15% (−930 ppm), due to a large SO (∼88 $cm^{-1}$) and relatively low $\Delta E$ (2.9 eV).

Substitution of F by Cl leads to an increase in $|\Delta g_\perp(\text{tot})|$ of about 4000 ppm (∼340% change) for $BX^+$, and of 2200 ppm (70%) for $AlX^+$. On the other hand, when replacing B by Al, $\Delta g_\perp$(tot) decreases by about −1600 ppm (−1630 vs −3260 ppm) in the fluorides, but increases slightly by ca. 100 ppm in the chlorides (≈−5600 vs −5500 ppm).

**Class III: BO, $BN^-$, BS, $BP^-$, AlO, $AlN^-$, $AlP^-$, and AlS.** The $g$ shifts of these radicals are more versatile, and therefore more difficult to rationalize, than those from classes I and II. There are several features which make class III radicals so distinctive.

(a) The SOS expansions of $\Delta g_\perp$ have large contributions from both $1^2\Pi_i$ and $2^2\Pi_r$ (whereas only $^2\Pi_r$ contributes strongly in classes I and II.) The $|L|$ values are small for $1^2\Pi_i$ (<0.3 au) but high for $2^2\Pi_r$ (∼1 au), in line with their spin-density distributions. Despite this, the $1^2\Pi_i$ coupling may be quite substantial when $\Delta E$ and SO are simultaneously small and large, respectively, a condition practically fulfilled by all AlX radicals of class III (Table 5). Also, as pointed out earlier, in class III the $^2\Pi_i$ state lies below $^2\Pi_r$.

(b) The $2^2\Pi_r$ contributions to $\Delta g_\perp$ are *negative* throughout (as in classes I and II), whereas those from $1^2\Pi_i$ are compound dependent: they are *negative* for boron but *positive* for aluminum radicals. Since the couplings with $1^2\Pi_i$ and $2^2\Pi_r$ are both *negative* for BX but, respectively, *positive* and *negative* for AlX, it is understandable why for class III radicals a general trend in the $g_\perp$ shifts cannot be established on a qualitative basis.

(c) The largest contributions to $\Delta g_\perp$ are due to $2^2\Pi_r$, except for $BN^-$, $AlN^-$, and $AlP^-$. Because of the small $\Delta E(1^2\Pi_i)$ values in these anions (0.2−0.9 eV), the $1^2\Pi_i$ coupling is stronger than that with $2^2\Pi_r$ (at variance with the behavior shown by most other nine VE radicals).

(d) The total $g_\perp$ shifts are negative, with the exceptions of $AlN^-$ and $AlP^-$, which surprisingly have positive $g_\perp$ values. In both anions, due to the energetic quasi-degeneracy between $X^2\Sigma^+$ and $1^2\Pi_i$, the positive contribution from $1^2\Pi_i$ surpasses, by far, the negative contribution from $2^2\Pi_r$. For $BN^-$, however, both states contribute negatively, so that the total perpendicular shift remains negative.

(e) Replacing O by S leads to a substantial increase of $|\Delta g_\perp|$, by about 6550 ppm for BO/BS and 4240 ppm for AlO/AlS. Surprisingly, AlS has a smaller $g_\perp$ shift than BS (−6915 vs

**TABLE 5: MRCI Values of $\Delta E$ (eV), SO ($cm^{-1}$), $L$ (au), and $\Delta g_\perp$ (ppm) for the $X^2\Sigma^+$ State of Boron and Aluminum Radicals $MX^{(-)}$ of Class III**

| $g$ shift | BO | $BN^-$ | BS | $BP^-$ | AlO | $AlN^-$ | $AlP^-$ | AlS |
|---|---|---|---|---|---|---|---|---|
| $\Delta g_{\parallel}$(tot) | −99 | −94 | −114 | −109 | −114 | −226 | −142 | −117 |
| $\Delta g_\perp$ | | | | | | | | |
| $1^2\Pi_i(1\pi)$ | | | | | | | | |
| $\Delta E$ | 3.530 | 0.881 | 2.474 | 1.188 | 1.000 | 0.322 | 0.177 | 0.895 |
| SO | 16.929 | 7.937 | −65.088 | 40.155 | 26.644 | 7.357 | 46.856 | 84.334 |
| $L$ | −0.259 | −0.251 | 0.235 | −0.216 | 0.165 | 0.404 | 0.156 | 0.079 |
| $\Delta g$ | −631 | −1150 | −3154 | −3620 | 2181 | 4572 | 20 492 | 3813 |
| $2^2\Pi_r(2\pi)$ | | | | | | | | |
| $\Delta E$ | 7.394 | 5.978 | 5.068 | 4.155 | 4.202 | 3.147 | 3.019 | 3.854 |
| SO | 16.426 | 7.569 | 43.920 | −34.236 | −37.596 | −23.823 | 53.364 | −64.554 |
| $L$ | −1.069 | −0.889 | −1.181 | 1.131 | 0.945 | 0.782 | −1.126 | 1.198 |
| $\Delta g$ | −1209 | −573 | −5212 | −4621 | −4193 | −2936 | −9874 | −10 222 |
| $(3-9)^2\Pi$ | | | | | | | | |
| $\Sigma\Delta g$ | 2 | −249 | −34 | 5 | −221 | −185 | −520 | −491 |
| Σ(2nd) | −1838 | −1972 | −8400 | −8236 | −2233 | 1451 | 10 098 | −6900 |
| 1st | −61 | −59 | −49 | −57 | −51 | −20 | −144 | −15 |
| $\Delta g_\perp$(tot) | −1899 | −2031 | −8449 | −8293 | −2284 | 1431 | 9954 | −6915 |
| $\langle\Delta g\rangle$ | −1300 | −1385 | −5670 | −5565 | −1560 | 880 | 6590 | −4650 |

−8450 ppm), contrary to what one would have expected for a second-row radical.

(f) The large $\Delta g_\perp$(BS) is caused by the negative contribution from $1^2\Pi_i$ (−3150 ppm), a state with small $L$ (0.235 au) but large SO ($\approx$−65 $cm^{-1}$). On the other hand, for AlS the $1^2\Pi_i$ contribution is quite similar to that of BS but *positive* (3800 ppm). Although in AlS the negative coupling with $2^2\Pi_r$ is about twice as large as for BS (−10 200 vs −5200 ppm), the different sign of the $1^2\Pi_i$ couplings results in $|\Delta g_\perp(\mathrm{BS})| > |\Delta g_\perp(\mathrm{AlS})|$. As seen in Table 5, the $g$ shifts of $BN^-$ are comparable with those of BO, and the same holds for BS and $BP^-$.

Unfortunately, few studies are available on off-diagonal matrix elements of $L$ and SO for comparison with our results. Sennesal et al.,[31] who carried out SCF plus limited CI calculations of the spin-rotation constant $\gamma$ of BS, reported for the $1^2\Pi_i$-$(1\pi)$ coupling $|L|$ and |SO| values of ∼0.20 au and 113 $cm^{-1}$, respectively, to be compared with MRCI results of 0.24 au and 65 $cm^{-1}$. For $2^2\Pi_r(2\pi)$, their $L$ and SO data are 0.88 au and 55 $cm^{-1}$ vs 1.18 au and 44 $cm^{-1}$ (MRCI, Table 5). The authors justified the large SO($1^2\Pi_i$) by a 5% contribution into $3\sigma$ from $p_\sigma$ of the S atom (large $\lambda$), besides 37% s and 58% $p_\sigma$ contributions from B (small $\lambda$).

According to ref 31, $\gamma$(BS) is dictated by the *negative* coupling with $1^2\Pi_i$ alone, and the same would then apply to $\Delta g_\perp$. On the other hand, CNDO results by Brom and Weltner[43] found that the $1^2\Pi_i$ coupling is small and *positive*, while that with $2^2\Pi_r(2\pi)$ is large and *negative*. In fact, our calculations show that both $^2\Pi$ states contribute substantially to $\Delta g_\perp$ (−3155 and −5210 $cm^{-1}$), so that a two-state coupling scheme is needed for $\Delta g_\perp$ and $\gamma$ of BS.

A similar shortcoming is found in the calculations of $\gamma$(AlO) by Mahieu et al.,[44] where only the $2^2\Pi_r$ coupling was considered. They reported for this state SO = 39 $cm^{-1}$ and $L_+ = 1.2$ au ($L \approx 0.85$ au), similar to ours. The interaction with $1^2\Pi_i$ was not included because they argued that its $L$ should be small (due to different spin-density localizations), an assumption corroborated by us (∼0.1 au). However, such a low $L$ value alone does not suffice to neglect the overall $1^2\Pi_i$ coupling since, as the MRCI results in Table 5 show, this state has a sizable contribution to $\Delta g_\perp$—mainly through the low $\Delta E$—and, therefore, to $\gamma$(AlO) as well.

An experimental estimate for $\langle X^2\Sigma^+|\mathrm{SO}|1^2\Pi_i\rangle$ of AlO is available. Analysis of local perturbations[45] between close-lying vibrational levels $1^2\Pi_i(v')-X^2\Sigma^+(v'')$ found such a matrix element to be −53 $cm^{-1}$ at the $R_c$ centroid (which is usually much larger than $R_e(X^2\Sigma^+)$). Further, taking a constant $L_+ = 0.5381$ au, and combining the SO value above with a second-order treatment for the (experimental) vibrational dependence of $\gamma$(AlO), it was found that SO varies almost linearly with $R$(Al−O). For example, at $R_e$ SO($1^2\Pi_i$) is about −8 $cm^{-1}$, indeed substantially less than −53 $cm^{-1}$, due to a shortening of $R$ by only 0.5 bohr. At $R_e$, we calculate SO ≈ 26 $cm^{-1}$ and $L \approx 0.15$ au.

Similarly, Coxon et al.[46] extracted $|\mathrm{SO}(1^2\Pi_i)| = 60.7$ $cm^{-1}$ from the optical spectrum of BO. This "experimental" value at $R \approx 3.3$ bohr may be compared with our MRCI result of 17 $cm^{-1}$ at $R_e$ (∼2.3 bohr), suggesting that SO($1^2\Pi_i$) also varies strongly with bond distance.

Apart from covalent contributions, two ionic structures are relevant to describe the bonding of class III radicals, namely, $M^+X^-$ and $M^{2+}X^{2-}$.[47] Obviously, ionic structures containing $X^{2-}$ do not contribute to the $MX^{(+)}$ halogenides of classes I and II.

For neutral radicals of class III, the lowest dissociation limit $M(^2P,s^2p) + X(^3P,s^2p^4)$ correlates, among others, with $X^2\Sigma^+$, $1^2\Pi_i$ and $2^2\Pi_r$ of MX. Here, in contrast with classes I and II, the M atom supplies a p orbital to the bonding, an important factor to achieve an effective magnetic coupling at that center.

On the other hand, the ionic products $M^+(^1S,s^2) + X^-(^2P,s^2p^5)$ generate the MX states $^2\Sigma^+(\sigma^2/\sigma\pi^4)$ and $^2\Pi_i(\sigma^2/\sigma^2\pi^3)$, while the double-ionic channel $M^{2+}(^2S,s) + X^{2-}(^1S,s^2p^6)$ gives rise to $^2\Sigma^+$-$(\sigma/\sigma^2\pi^4)$ only. Other higher-lying ionic channels include $M^+$-$(^3P,sp) + X^-$ and $M^{2+}(^2P,p) + X^{2-}$, both generating $^2\Sigma^+$ and $^2\Pi$ states of MX. This simple analysis indicates that the bonding in the $X^2\Sigma^+$ and $1,2^2\Pi$ states of class III radicals is expected to be quite polar.

Indeed, ab initio studies[47] on AlO have found that $X^2\Sigma^+$ changes its structure from $Al^{2+}O^{2-}$ to $Al^+O^-$ between $R = 3.0$ bohr and $R = 4.0$ bohr (note that $R_e = 3.057$ bohr, Table 2). Extensive calculations by Zenouda et al.[47] reported electric-dipole $\mu_e$ values (D) of 4.24, 1.45, and 3.18 for $X^2\Sigma^+$, $1^2\Pi_i$, and $2^2\Pi_r$, respectively, i.e., a highly polar bond in $X^2\Sigma^+$ and $2^2\Pi_r$ but a less polar one in $1^2\Pi_i$ (all with $Al^{(+)}O^{(-)}$ polarity). In any case, the polar bonding explains why the $1^2\Pi_i$ states in class III radicals have bound potentials (whereas they are repulsive in classes I and II). The $\mu_e$ values of BO follow the same trend.[48] The radicals BS and AlS, for which such ab initio data are not available, probably also have large $M^+S^-$ and $M^{2+}S^{2-}$ contributions.

**TABLE 6: Summary of Theoretical and Experimental Δ*g* Data (ppm) for Classes I and II Radicals[a]**

| radical | ref | $\Delta g_{\parallel}$ | $\Delta g_{\perp}$ | $\langle\Delta g\rangle$ |
|---|---|---|---|---|
| | | Class I | | |
| BeF | tw | −50 | −823 | −565 |
| | exptl[38] | −900 ± 500 | −900 ± 500 | −900 ± 500 |
| $BeO^-$ | tw | −36 | −1504 | −1015 |
| BeCl | tw | −55 | −3128 | −2104 |
| | exptl[52] | −1300 ± 1000 | −4300 ± 1000 | −3300 ± 1000 |
| MgF | tw | −54 | −1809 | −1224 |
| | 8 | −59 | −1447 | −984 |
| | 50 | −60 | −2178 | −1472 |
| | 51a | −20 | −1314 | −869 |
| | exptl[53] | −300 ± 500 | −1300 ± 500 | −950 ± 500 |
| $MgO^-$ | tw | −49 | −2511 | −1690 |
| MgCl | tw | −61 | −4264 | −2863 |
| CaF | 20 | −42 | −2980 | −2001 |
| | exptl[53] | −300 ± 500 | −2300 ± 1000 | −1600 ± 1000 |
| | | Class II | | |
| $BF^+$ | tw | −108 | −1633 | −1125 |
| | exptl[54] | −1100 ± 300 | −1900 ± 300 | −1600 ± 300 |
| $BCl^+$ | tw | −117 | −5620 | −3786 |
| $AlF^+$ | tw | −109 | −3263 | −2212 |
| | exptl[55] | −800 ± 500 | −2300 ± 500 | −1800 ± 500 |
| $AlCl^+$ | tw | −118 | −5490 | −4433 |

[a] Results for CaF are also included. tw = this work.

**TABLE 7: Summary of Theoretical and Experimental Δ*g* Data (ppm) for Class III Radicals[a]**

| radical | ref | $\Delta g_{\parallel}$ | $\Delta g_{\perp}$ | $\Delta g$ |
|---|---|---|---|---|
| BO | tw | −99 | −1899 | −1299 |
| | 50 | −72 | −2298 | −1556 |
| | exptl[56a] | −800 ± 300 | −1100 ± 300 | −1000 ± 300 |
| | exptl[56b] | −300 ± 400 | −1700 ± 300 | −1200 ± 300 |
| $BN^-$ | tw | −94 | −2031 | −1385 |
| BS | tw | −114 | −8449 | −5671 |
| | 50 | −83 | −9974 | −6677 |
| | exptl[43] | −700 ± 100 | −8200 ± 100 | −5700 ± 100 |
| $BP^-$ | tw | −109 | −8293 | −5565 |
| AlO | tw | −114 | −2284 | −1560 |
| | 50 | −142 | −222 | −195 |
| | exptl, Ne[57a] | −800 ± 300 | −1900 ± 300 | −1500 ± 300 |
| | exptl, Ar[57a] | −900 ± 300 | −2600 ± 500 | −2000 ± 300 |
| | exptl, Kr[57a] | −3000 ± 500 | −5000 ± 500 | −4430 ± 500 |
| | exptl, Ne[57b] | −300 ± 200 | −1200 ± 200 | −900 ± 200 |
| $AlN^-$ | tw | −226 | 1431 | *880* |
| AlS | tw | −121 | −6915 | −4649 |
| $AlP^-$ | tw | −142 | 9954 | *6589* |

[a] tw = this work.

In brief, low-lying states of class III radicals are described by a mixing of MX, $M^+X^-$, and $M^{2+}X^{2-}$ configurations. Since the SO ($L$) matrix elements between GS and the $^2\Pi$ manifold depend on the relative weight of each configuration but such weights vary substantially with $R$(M−X), the strong distance dependence of SO($1^2\Pi_i$) observed experimentally for AlO is understandable.[45] The same behavior is expected for other diatomics of class III.

### Discussion of the Calculated *g* Shifts

Table 6 summarizes the theoretical Δ*g* values (from this work and the literature) for classes I and II radicals, while Table 7 collects those for class III. Experimental data (rare-gas matrix) are also included. The MRCI isotropic shifts $\langle\Delta g\rangle = (\Delta g_{\parallel} + 2\Delta g_{\perp})/3$ of neutral and positive ions are displayed diagrammatically in Figure 1. Since all theoretical $\Delta g_{\parallel}$ values are rather small, each $\langle\Delta g\rangle$ is practically equal to $(2/3)\Delta g_{\perp}$.

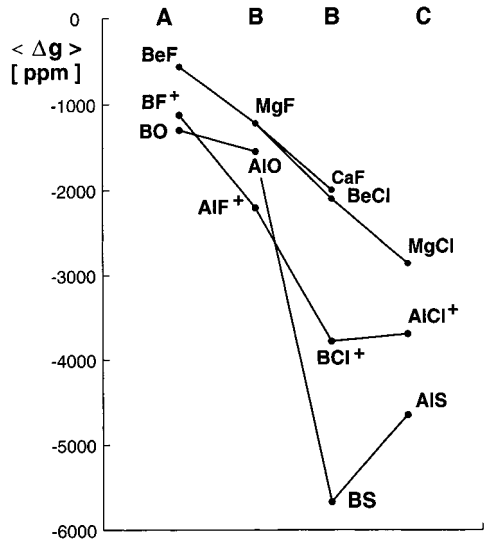


**Figure 1.** Diagrammatic representation of the MRCI isotropic shifts $\langle\Delta g\rangle$ for radicals $MX^{(+)}$ from classes I−III. The set labeling A−C is given at the top of the figure.

The theoretical $|\langle\Delta g\rangle|$ values (ppm) increase in the following orders.

class I (−570 to −2865): BeF < $BeO^-$ < MgF < $MgO^-$ < BeCl < MgCl [A < A < B < B < B < C]

class II (−1125 to −3790): $BF^+$ < $AlF^+$ < $BCl^+$ ≈ $AlCl^+$ [A < B < B ≈ C]

class III (−1300 to −5670): BO ≈ $BN^-$ < AlO < AlS < $BP^-$ ≈ BS [A ≈ A < B < C < B ≈ B]

$AlN^-$ and $AlP^-$, with $\langle\Delta g\rangle$ values of about 900 and 6600 ppm, respectively, behave anomalously, and have been excluded in the above comparison.

For classes I and II the ordering of $\langle\Delta g\rangle$ with respect to sets, A < B < C, can be considered as the normal—and expected—trend, with the isotropic Δ*g* value for mixed-row radicals of set B lying between those of sets A and C.

However, the ordering for class III is somewhat abnormal. For instance, AlS from set C has a smaller $\langle\Delta g\rangle$ than those of BS and $BP^-$ (both set B), contrary to expectations, since the atomic $\lambda$ values increase by about 1 order of magnitude between $B^{(1+,2+)}$ and $Al^{(1+,2+)}$.[36,37] In fact, BS and $BP^-$ have the largest *negative* $\langle\Delta g\rangle$ values among all radicals investigated here.

The different behavior of BX and AlX radicals of class III is evident: while BO and $BN^-$ from set A have similar $\langle\Delta g\rangle$ values—and the same holds for BS/$BP^-$ from set B—the pair AlS and $AlP^-$ from set C have very little in common, as pointed out by $\langle\Delta g\rangle$ values of opposite sign (−4650 vs 6590 ppm, Table 7).

Further trends regarding $\langle\Delta g\rangle$ are the following.

For each set, $|\langle\Delta g\rangle|$ generally increases along the class sequence I → II → III, namely, BeF < $BF^+$ < BO for set A, and similarly for the triads starting with BeCl (set B) and MgCl (set C). However, the different ordering MgF (I) < AlO (III) < $AlF^+$ (II) from set B indicates that $|\Delta g_{\perp}|$ is either too small for AlO or too large for $AlF^+$. However, as seen in Figure 1, a quasi-linear relationship for the $\langle\Delta g\rangle$ values of $BF^+$, $AlF^+$, and $BCl^+$ suggests that $AlF^+$ behaves normally, and therefore, AlO-(III) seems to be out of place.

**TABLE 8: Comparison of the Spin-Rotation Constants $\gamma$ and $\Delta g_\perp$ Values for BO, BS, AlO, AlS, and MgCl As Obtained via the Curl Equation[a]**

| radical | exptl $\gamma_v$ ($cm^{-1}$) [estimated $\Delta g'_\perp$, ppm] | estimated $\gamma'_0$ ($cm^{-1}$) [$\Delta g_\perp$, ppm] |
|---|---|---|
| BO ($B = 1.556\ cm^{-1}$) | $\gamma_0 = 0.005\ 96$ [−1915] mw[69] | $\gamma' = 0.0034$ [−1100, exptl][56a] |
| | | $\gamma' = 0.0053$ [−1700, exptl][56a] |
| | $\gamma_0 = 0.003\ 62$ [−1160] opt[70] | |
| | $\gamma_2 = 0.0065$ [−2090] opt[71] | $\gamma' = 0.0059$ [−1899, th] [tw] |
| | | $\gamma' = 0.0072$ [−2298, th][50] |
| | $\gamma_0 = 0.004\ 91$ [−1580] opt[46] | |
| | $\gamma_1 = 0.005\ 06$ [−1625]; $\gamma_2 = 0.005\ 33$ [−1715]; $\gamma_3 = 0.005\ 11$ [−1645]; $\gamma_4 = 0.005\ 65$ [−1815] | |
| BS ($B = 0.707\ cm^{-1}$) | $\gamma_0 = 0.0132$ [−9300] mw[72] | $\gamma' = 0.0116$ [−8200, exptl][43] |
| | $\gamma_0 = 0.013(2)$ [−9200 ± 1400] opt[73a] | $\gamma' = 0.0120$ [−8449, th] [tw] |
| | $\gamma_0 = 0.0136$ [−9600] opt[73b] | $\gamma' = 0.0141$ [−9974, th][50] |
| | | $\gamma' = 0.0127$ (ab initio[31]) |
| AlO ($B = 0.593\ cm^{-1}$) | $\gamma_0 = 0.001\ 73$ [−1460] mw[61a] | $\gamma' = 0.002\ 25$ [−1900, exptl][57a] |
| | $\gamma_0 = 0.001\ 723$ [−1450] mw[61b] | $\gamma' = 0.003\ 08$ [−2600, exptl][57a] |
| | | $\gamma' = 0.0156$ [−5000, exptl][57a] |
| | $\gamma_0 = 0.0050$ [−4200] opt[44] | $\gamma' = 0.001\ 42$ [−1200, exptl][57b] |
| | $\gamma_1 = 0.0061$ [−5140]; $\gamma_2 = 0.0060$ [−5060] | |
| | | $\gamma' = 0.002\ 71$ [−2284, th] [tw] |
| | $\gamma_0 = 0.001\ 723$ [−1450] mw[45] | $\gamma' = 0.000\ 26$ [−222, th][50] |
| | $\gamma_1 = 0.000\ 530$ [−445]; $\gamma_2 = 0.001\ 05$ [885] | |
| | $\gamma_0 = 0.001\ 723$ [−1450] opt[62] | |
| | $\gamma_1 = 0.000\ 033$ [30]; $\gamma_2 = 0.000\ 66$ [−560] | |
| | $\gamma_3 = 0.002\ 91$ [−2455] | |
| AlS ($B = 0.255\ cm^{-1}$) | $\gamma_0 = 0.002\ 20$ [−4315] mw[59] | $\gamma' = 0.0035$ [−6915, th] [tw] |
| | $\gamma_0 = 0.0043$ [−8430] opt[74] | |
| | $\gamma_0 = 0.002\ 20$ [−4315] opt[60] | |
| | $\gamma_1 = 0.001\ 00$ [−1960]; $\gamma_2 = 0.000\ 15$ [290] | |
| | $\gamma_3 = 0.000\ 50$ [−985] | |
| MgCl ($B = 0.248\ cm^{-1}$) | $\gamma_0 = 0.002\ 22$ [−4475] mw[40a] | $\gamma' = 0.002\ 11$ [−4264, th] [tw] |
| | $\gamma_0 = 0.002\ 12$ [−4275] mw[40b] | |

[a] th = theoretical. tw = this work.

For each class, chlorides and sulfides have larger $\langle \Delta g \rangle$ values than the corresponding fluorides and oxides, as expected from their atomic $\lambda$ values. This trend demonstrates again that the $3\sigma$ SOMO, besides its predominant $sp_\sigma(M)$ composition, also has an admixture of $p_\sigma(X)$, giving rise to larger SO values. While such a feature could have been expected for the more covalent radicals of class III, it is less evident for those from the ionic-like classes I and II.

Class I seems to be the only one having a "normal" behavior with respect to different criteria: First, it shows an almost linear relationship among its members, a feature supported when CaF is included (Figure 1). Second, the ordering BeF < MgF < CaF—and a similar one for BeCl and MgCl—correlates well with $\lambda$ increasing from Be to Ca.

As seen in Figure 1, $\langle \Delta g \rangle$ of CaF lies between those of MgF and BeCl. For the series BeF → MgF → CaF, the $\Delta g_\perp$ value decreases on average by −1000 ppm in each step, and for BeCl → MgCl, by ≈−1100 ppm. On the basis of this trend, $\Delta g_\perp$(CaCl) is expected to lie near −5300 ppm. Experimental ESR lines centered at $g = 1.998(1)$, or $\langle \Delta g \rangle \approx -4300(\pm 1000)$ ppm, were tentatively assigned to CaCl,[49] an assumption supported by our extrapolated value.

On the other hand, class II shows a mixed behavior: substitution of B by Al gives the expected increase in $|\langle \Delta g \rangle|$ for the fluorides ($BF^+ < AlF^+$), but not for the chlorides ($BCl^+ \approx AlCl^+$). Further, while class III oxides (BO < AlO) behave like class II fluorides ($BF^+ < AlF^+$), the corresponding sulfides (AlS < BS) deviate from the chlorides, as exemplified by $|\langle \Delta g \rangle|$ of BS being about 1000 ppm larger than that of AlS (Figure 1).

Our study reveals the reasons behind the peculiar behavior shown by class III radicals: $1^2\Pi_i$ and $2^2\Pi_r$ both contribute *negatively* to $\Delta g_\perp$ of BO, $BN^-$, $BP^-$, and BS, but *positively* and *negatively*, respectively, to $\Delta g_\perp$ of AlO, $AlN^-$, $AlP^-$, AlS. Thus, the two $^2\Pi$ contributions enhance each other in BX but mutually cancel in AlX.

The situation becomes more acute for $AlP^-$, where a very large positive contribution of ∼20 500 ppm from $1^2\Pi_i$ dominates, due to a rather small $\Delta E$ of 0.18 eV. If this $\Delta E$ were as high as for AlO and AlS (∼0.9 eV), then the $1^2\Pi_i$ coupling would have been about 5 times smaller (∼4100 ppm), and $\Delta g_\perp$(tot) of $AlP^-$ negative. The same argument applies to $AlN^-$.

### Comparison with Experimental Data

In this section, our calculated $g$ shifts are compared with experimental results from ESR studies in matrices (Tables 6 and 7), as well as with $\Delta g_\perp$ data estimated, via Curl's equation, from gas-phase spin-rotation constants (Table 8).

**Matrix *g* Data.** The ESR spectra—available for about half of the present 18 radicals—show that the $\Delta g_\parallel$ and $\Delta g_\perp$ values are negative. This trend is reproduced by our results. It is found to hold as well for those diatomics not yet observed experimentally, except for $AlN^-$ and $AlP^-$, which are predicted to have positive $\Delta g_\perp$ values (about 1400 and 10 000 ppm).

The calculated $\Delta g_\parallel$ values, which are small (≈−100 ppm) and practically independent of the compound, deviate to a large extent from the experimental data (−600 ppm on average), a discrepancy also found in previous $g$ factor calculations.[50,51] Matrix effects are partly responsible for such large $\Delta g_\parallel$ values.[3] It should also be noted that the measured values are affected by uncertainities up to 50%.

The $\Delta g_\perp$ components are significantly larger (−800 to −8500 ppm), and change substantially from one compound to another. The calculated $\Delta g_\perp$ values generally reproduce the experimental trends quite well (perhaps with the exception of AlO; see below), a remarkable agreement since our results do not include vibrational averaging.

The ESR spectrum[38] of BeF gives $\Delta g_{\parallel} \equiv \Delta g_{\perp} = -900$ ppm, with a large error of ±500 ppm. Due to a discrepancy for $A_{dip}$-($^{19}$F) between experiment and theory, BeF was found to be free rotating in the matrix, as also suggested by the isotropy of $\Delta g$. Our results, $\Delta g_{\parallel} = -50$ and $\Delta g_{\perp} = -820$ ppm (close to the observed value), show that the $g$ shifts are indeed not isotropic.

For BeCl, within experimental error bounds of ±1000 ppm, our calculated $g_{\perp}$ shift of −3130 ppm seems reasonable (−4300 ppm in matrices[52]). The measured shift is about 5 times larger than that of BeF; the MRCI calculations reproduce such a trend, but by a factor of only 4. Because of a large experimental $\Delta g_{\parallel}$ of −1300(±1000) ppm, there is a large discrepancy between measured and calculated $\langle \Delta g \rangle$ values.

An ESR study[53] on MgF gives $\Delta g_{\perp} = -1300(\pm 500)$ ppm, only 400 ppm below that of BeF. The experimental $\langle \Delta g \rangle = -950(\pm 500)$ ppm is reproduced reasonably well by all theoretical values, ranging from −870 to −1475 ppm.

We are unaware of any experimental $\Delta g$ for MgCl. However, due to the good performance of our calculations for other class I radicals, and the quasi-linear variation shown in Figure 1, an MRCI $\langle \Delta g \rangle \approx -2900$ ppm is considered to be quite reliable.

For the cations $MX^+$ of class II, experimental $\Delta g$ values are available only for $BF^+$ [54] and $AlF^+$.[55] Since these radicals have a strong mixing $^2\Pi_i$–$^2\Pi_r$ in the Franck−Condon region,[30,32] the magnetic coupling is expected to be rather sensitive to $R$(M−X). Taking this fact into account, our calculations at $R_e$ reproduce the experimental observations fairly well.

For BO, there is also good agreement between theory and experiments,[56] in particular for the latest reported $\Delta g_{\perp}$ value of −1700 ppm (Table 7). The DFT result[50] appears to be too large. Similar observations hold for BS.

The largest discrepancy is found for AlO. First, the strong matrix effects shown by $\Delta g_{\perp}$, which, according to a 1971 study by Knight et al.,[57a] varies from −1900 to −2600 to −5000 ppm in Ne, Ar, and Kr matrixes, respectively, should be pointed out. Also, a $\Delta g_{\parallel}$ value of −3000 ppm in Kr is not "small". Such substantial matrix shifts most probably originate in the high polarity of AlO ($\mu_e = 4.2$ D), resulting in an increase in guest−host interactions as the host atoms become more polarizable. Later, a 1997 reinvestigation by Knight et al.[57b] for AlO in Ne matrixes reported smaller $g$ shifts, −300 ppm for $\Delta g_{\parallel}$ and −1200 ppm for $\Delta g_{\perp}$, combined with a better accuracy (±200 ppm).

An MRCI-calculated $\Delta g_{\perp}$(AlO) of −2284 ppm is in good to reasonable accord with the Ar and old Ne data, but not at all with the new Ne study, which gives values for $\Delta g_{\perp}$ and $\langle \Delta g \rangle$ about half of ours. (Please note that in the present work we have used a slightly different strategy than earlier, where we obtained $\Delta g_{\perp} = -2675$ ppm.[20] Now, for the NOs and $g$ shifts, the wave functions of the two lowest $^2\Sigma^+$ states were calculated simultaneously.)

The DFT method, as pointed out in ref 49, fails completely for $\Delta g_{\perp}$(AlO): a calculated value of −220 ppm is 1 order of magnitude too small. As an explanation for such a discrepancy, the authors speculated about the possible failure of second-order perturbation theory when dealing with the $g$ shifts of second- and higher-row radicals. We have shown elsewhere that such an argument is not valid.[20] Since the descriptions of the ground and low-lying states of AlO require multireference treatments,[57a] the DFT approach might not be flexible enough in this case. On the other hand, the DFT results for BS, a set B radical like AlO, can be considered as adequate (Table 7).

**$\Delta g_{\perp}$ Data from Gas-Phase Spin-Rotation Constants.** Approximate $\Delta g_{\perp}$ vallues can be derived from spin-rotation constants $\gamma$, and vice versa. Curl's equation[3,58] relates $\Delta g_{\perp}$ and $\gamma$ values of $^2\Sigma^+$ states according to the expression $\Delta g_{\perp} = -\gamma/2B$, where $B$ represents an average rotational constant for $X^2\Sigma^+$ and $1,2^2\Pi$ states. Experience from the literature[3,58] shows that the so-calculated $\Delta g_{\perp}$ lies within ±10% of the experimental value. Interestingly, measurement in the gas phase of $\gamma_v$ as a function of vibrational level $v$ allows the $v$ dependency $(\Delta g_{\perp})_v$ to be estimated as well, which is difficult, if not impossible, to obtain directly from matrix ESR studies.

Gas-phase $\gamma$ values—available only for MgCl, BO, BS, AlO, and AlS—are compiled in Table 8. The column "exptl $\gamma_v$" lists microwave (mw) and optical (opt) values, while $g_{\perp}$ shifts (in brackets) derived from $\gamma$ using Curl's equation are denoted as $\Delta g'_{\perp}$. The last column lists $\gamma$ values calculated from experimental and theoretical $\Delta g_{\perp}$ data; they are denoted as $\gamma'$. For the radicals not covered in Table 8, most of class I and all of class II, approximate $\gamma$ values can be estimated using the $\Delta g_{\perp}$ data from Table 6.

Experimental $\gamma$ values from different sources are in good accord which each other for BX but not for AlX systems. (mw studies are considered to give the most accurate $\gamma$ values.) As well, the $\gamma'$ values of BO and BS calculated from matrix $\Delta g_{\perp}$ values cover a range similar to that of the gas-phase $\gamma_0$ values, supporting Curl's equation. This, however, is not the case for aluminum radicals, for which the ESR $\Delta g_{\perp}$ values correspond to $\gamma'$ values generally larger than the experimental $\gamma_0$ values (Table 8). The possible reasons for such deviations will be discussed later.

An MRCI value of −1900 ppm for $\Delta g_{\perp}$(BO) agrees with −1915 and −2090 ppm derived from the mw $\gamma_0$ values and one opt $\gamma_0$ value. Two other optical $\gamma_0$ values give a smaller $\Delta g'_{\perp}$ (−1160 and −1580 ppm). Overall, these results favor a matrix $\Delta g_{\perp}$ value of −1700 ppm over a smaller one of −1100 ppm. On the basis of a study[46] reporting $\gamma_v$ for $v = 0-4$, $\Delta g'_{\perp}$(BO) should change little in that region (−1580 to −1815 ppm).

Our theoretical $\Delta g_{\perp} = -8450$ ppm for BS lies within 10% of $\Delta g'_{\perp} = -9300$ ppm; both are in good agreement with a matrix result of −8200 ppm. The DFT study also reproduces the experimental trend. For BS, like BO, both $1^2\Pi_i$ and $2^2\Pi_r$ contribute negatively to $\Delta g_{\perp}$, or positively to $\gamma$. For AlO and AlS, contrastingly, their respective contributions are of opposite sign. Because of this, $\gamma_0$(BS) is 1 order of magnitude larger than $\gamma_0$(AlO).

There are no ESR data for AlS, so we can only compare an MRDCI $\Delta g_{\perp} = -6915$ ppm with $(\Delta g'_{\perp})_0 \approx -4315$ ppm from a mw work.[59] Optical studies[60] indicate that $\gamma_v$ depends strongly on $v$, as in AlO, which will be discussed next in some detail.

AlO is more complicated since contradictory experimental values have been reported for $\gamma$, and, as pointed out earlier, for $\Delta g_{\perp}$ as well. Two independent microwave studies[61] found $\gamma_0 \approx 0.001\,72$ cm$^{-1}$ ($\Delta g'_{\perp} \approx -1450$ ppm), much smaller than an optical value[44] of 0.0050 cm$^{-1}$ ($\Delta g'_{\perp} \approx -4200$ ppm). On the other hand, the matrix $\Delta g_{\perp}$ values range from −1200 to −5000 ppm ($\gamma'$ from about 0.0014 to 0.0156 cm$^{-1}$), while theory predicts −222 ppm (DFT) and −2285 ppm (this work), corresponding to $\gamma'$ values of 0.000 26 and 0.002 71 cm$^{-1}$. Certainly, AlO appears to be a sensitive case for both experiment and theory.

The variation of $\gamma$(AlO) with $v$ has been studied (Table 8). In the mw work,[45] $\gamma_v$ *decreases* by 0.002 77 cm$^{-1}$ between $v = 0$ and $v = 2$, thereby becoming negative for $v = 2$. Using these data, Curl's equation gives $\Delta g'_{\perp} \approx 900$ ppm for $v = 2$ versus $\Delta g'_{\perp} \approx -1450$ ppm for $v = 0$. In other words, for $v = 2$ the *positive* contribution to $\Delta g_{\perp}$ from $1^2\Pi_i$ surpasses the

**TABLE 9: Contributions of $1^2\Pi$ and $2^2\Pi$ to $\Delta g_\perp$ for Selected Diatomics with Nine Valence Electrons, All Having a $X^2\Sigma^+(1\pi^4 3\sigma)$ Ground State[a]**

| | BeF, $BeO^-$, BeCl, MgF, $MgO^-$, MgCl, $BF^+$, $BCl^+$, $AlF^+$ | $AlCl^+$ BO, $BN^-$, BS, $BP^-$ | AlO, AlS | $AlN^-$, $AlP^-$ |
|---|---|---|---|---|
| $^2\Pi_i(1\pi)$ | $2^2\Pi$ | $1^2\Pi$ | $1^2\Pi$ | $1^2\Pi$ |
| $\Delta g_\perp(^2\Pi_i)$ | small (negative or positive) | negative | positive | positive |
| | −150 to +400 | −600 to −5700 | 2000−3800 | 4600−20500 |
| $^2\Pi_r(2\pi)$ | $1^2\Pi$ | $2^2\Pi$ | $2^2\Pi$ | $2^2\Pi$ |
| $\Delta g_\perp(^2\Pi_r)$ | negative | negative | negative | negative |
| | −700 to −5800 | −600 to −3600 | −4400 to −10 200 | −3300 to −9900 |
| $\Delta g_\perp$(tot) | negative | negative | negative | positive |
| | −800 to −6600 | −1800 to −8400 | −2600 to −6900 | 1400 to 10000 |

[a] Numbers are $\Delta g_\perp$ values (ppm).

*negative* one from $2^2\Pi_r$. An optical study[62] finds a similarly strong vibrational dependency for $\gamma_v$(AlO).

As shown by Ito et al.,[45] the peculiar $v$ dependency of $\gamma_v$(AlO) is governed by the coupling with the close-lying $1^2\Pi_i$ (e.g., $1^2\Pi_i(v=0)$ lies about 0.3 eV above $X^2\Sigma^+(v=2)$). Because of the a quasi-degeneracy $X^2\Sigma^+/1^2\Pi_i$, any changes of $\Delta E$ lead to large variations in $\Delta g_\perp$. Also, the SO and $L$ values are expected to vary substantially with geometry, due to the heavy mixing of AlO, $Al^+O^-$, and $Al^{2+}O^{2-}$ structures near $R_e$.

## Summary and Concluding Remarks

The electron-spin $g$ shifts of eighteen $X^2\Sigma^+(1\pi^4 3\sigma)$ radicals $MX^{(\pm)}$ with nine VEs have been calculated using a second-order perturbation treatment, a Hamiltonian based on Breit−Pauli theory, and MRCI(NO) wave functions. To date, ESR spectra are only available for eight of these systems. In our study, besides reporting the $g$ shifts of a larger number of radicals, we also find some unexpected and interesting results, worthy of future experimental undertakings.

The second-order contributions to $\Delta g_\perp$ due to $^2\Pi_i(1\pi\rightarrow 3\sigma)$ and $^2\Pi_r(3\sigma\rightarrow 2\pi)$, which dominate the SOS expansions, are summarized in Table 9. These two terms may have the same or opposite sign, leading to enhanced or reduced $\Delta g_\perp$(tot) values. Total values can be positive or negative. As shown below, several factors are responsible for such a variety in $\Delta g_\perp$ values.

For class III radicals (BO, AlO, $AlN^-$, ...), the inverted $^2\Pi_i$ is the lowest state of this symmetry, followed by the regular $^2\Pi_r$. In classes I and II (BeF, $BF^+$, ...), the ordering is the opposite, with the exception of $AlCl^+$ (class II) showing the same pattern as class III systems.

The $^2\Pi_i(1\pi\rightarrow 3\sigma)$ contribution to $\Delta g_\perp$, according to a simple rule assumed to hold for doubly occupied MO → SOMO excitations, should be positive.[3] We find this to be valid in most cases, but not for $AlCl^+$ (class II) and BX radicals (class III), where it is negative. On the other hand, the $^2\Pi_r$ couplings are calculated to always be negative, in line with expectations for SOMO → virtual MO excitations.[3]

Each $^2\Pi$ contribution to $\Delta g_\perp$ is proportional to $(SO)L(\Delta E)^{-1}$. The coupling with $^2\Pi_r(2\pi)$ is dominated by its large SO and $L$, as both $3\sigma$ and $2\pi$ are localized on atom M—with $\Delta E$ playing a secondary role. Contrastingly, the $^2\Pi_i(1\pi)$ coupling is determined by $\Delta E$, as both SO and $L$ are generally small because of the different spin localizations of $1\pi$(X) and $3\sigma$(M). Only in class III—where $\Delta E(1^2\Pi_i)$ is low—is this coupling important. Models in which only one $^2\Pi$ state was used are certainly inappropriate for class III radicals.[31,44]

As seen in Table 9, for the first group of radicals—class I and most of class II—the contribution from $^2\Pi_i$ is negligible, since in addition to small SO and $L$, this state is not the lowest one. The overall $\Delta g_\perp$ is therefore negative, due to $^2\Pi_r$. For the second group—mainly BX radicals—the $^2\Pi_i$ state is the lowest-lying [large $(\Delta E)^{-1}$ factor], but its contribution is negative (contrary to the rule), so $\Delta g_\perp$ has two large negative components. For the third group—AlO and AlS—the lowest $^2\Pi_i$ contributes positively, thereby partly compensating for the negative coupling with the higher-lying $^2\Pi_r$. For the last group—$AlN^-$ and $AlP^-$—due to its very low energy, the positive $^2\Pi_i$ contribution outweighs the negative one from $^2\Pi_r$, resulting in a positive $\Delta g_\perp$(tot), whereas all other radicals have negative values for such a component.

As shown in previous sections, a qualitative prediction as to the sign and approximate $\Delta g_\perp$ value is very difficult. Interesting situations arise. For example, since for BO, $BN^-$, BS, and $BP^-$ the $1^2\Pi_i$ and $2^2\Pi_r$ states both act in the same direction (*negatively*), the total $\Delta g_\perp$ values are comparatively larger than expected for the atoms M involved. The pair BS/AlO from set B is a case in point: ESR studies[43,57] reported a $\Delta g_\perp$ (ppm) of −8200 for BS but, depending on the matrix, from −1200 to −5000 for AlO, despite $\lambda(\mathrm{Al}) \approx 10\lambda(\mathrm{B})$. In fact, as seen in Table 9, the $g_\perp$ shifts of BX and AlX radicals from class III have very little in common.

From a theoretical point of view, AlX (class III) compounds are more difficult to handle because of the delicate balance between positive and negative terms. (The same holds for $H_2CO^+(X^2B_2)$,[63] where a small positive $\Delta g_{zz}$(tot) arises from a large and positive contribution, due to $^2B_1(\pi\rightarrow n)$, being counterbalanced by another one of similar magnitude but negative, due to $^2B_1(n\rightarrow\pi^*)$). The $\Delta g_\perp$ values of the other MX radicals are easier to calculate since the coupling with just one $^2\Pi$ state dominates (classes I and II), or the couplings with the two $^2\Pi$ states have the same sign (BX in class III).

In physical terms, for negative $g_\perp$ shifts (here, from −800 to −8500 ppm), the magnetic moments are smaller than that of a free electron; i.e., the magnetic coupling of $X^2\Sigma^+$ with the $^2\Pi$ manifold leads to an effective loss of spin angular momentum. For $AlN^-$ and $AlP^-$, which are predicted to have *positive* $\Delta g_\perp$ values (about 1400 and 10 000 ppm), the magnetic moments are larger. The main reason for such "anomalous" $\Delta g_\perp$(tot) > 0 lies in the quasi-degeneracy ($\Delta E \approx 0.3$ eV) of $X^2\Sigma^+(1\pi^4 3\sigma)$ and $1^2\Pi_i(1\pi^3 3\sigma^2)$, with the $3\sigma$ unpaired electron acquiring additional orbital angular momentum due to its strong SO mixing with $1\pi$.

The $\Delta g_\perp$ values of classes I and II radicals no only are of similar magnitude but also behave more regularly than those of class III. Besides the reversed order of stabilities between the $^2\Pi_r$ and $^2\Pi_i$ states, the differences between class I/II and class III radicals relate to the composition of $X^2\Sigma^+$ near equilibrium.

(a) The GSs for classes I and II radicals are mostly described by *one* ionic structure, $M^+(\sigma)X^-(\sigma^2\pi^4)$ and $M^{2+}(\sigma)X^-(\sigma^2\pi^4)$,

respectively. The lowest dissociation products, $M(\sigma^2)X(\sigma\pi^4)$ for class I and $M^+(\sigma^2)X(\sigma\pi^4)$ for class II, also make some contribution. The similarity in bonding in both classes thus justifies the uniformity of their $\Delta g_\perp$ values.

Most importantly, mutual polarization between $M^+$ and $X^-$ in class I, or between $M^{2+}$ and $X^-$ in class II, results in $3\sigma$ having $sp_\sigma$ contributions from M (low $\lambda$) *as well as* X (large $\lambda$).[64] Due to this X contribution, the coupling of $X^2\Sigma^+$ with $1^2\Pi_r$-$(2\pi)$—which practically determines the total $\Delta g_\perp$ values in both classes—is somewhat larger than expected for unpaired electrons localized at centers with small $\lambda$ values (Be, Mg, B, Al).

(b) The GS in class III is described by *two* ionic structures, $M^+(\sigma^2)X^-(\sigma\pi^4)$ and $M^{2+}(\sigma)X^{2-}(\sigma^2\pi^4)$, plus covalent ones from M + X products, $M(\sigma^2\sigma)X(\pi^4)$ and $M(\sigma^2\sigma)X(\sigma^2\pi^2)$. Here, $3\sigma$, $1\pi$, and $2\pi$ MOs consist of more balanced linear combinations of M and X AOs than those for classes I and II radicals, thereby increasing the $p_\sigma(X)$ contribution to the SOMO. Also, the $M(s^2p)$ atom effectively contributes $p_\sigma$ to the MX bond—besides those due to $sp_\sigma$ hybridization in $M^+(\sigma^2)$ and $M^{2+}(\sigma)$. In brief, the enhanced amount of $p_\sigma(M$ *and* $X)$ in $3\sigma$ leads to the larger $\Delta g_\perp$ values calculated for class III radicals.

The importance of $p_\sigma$ contributions to the SOMO in determining the $\Delta g_\perp$ values can be seen by comparing the radicals studied here with other diatomics. For example, the $\Delta g_\perp$ values for nine VE systems are found to be much larger than those calculated (ca. $-100$ ppm) for the $X^2\Sigma_{(g,u)}^+$ radicals $Li_2^+$, $Li_2^-$, and $Be_2^+$ with one or three VEs.[5] Such low $g_\perp$ shifts are characteristic of SOMOs having a predominant s composition, and constituent atoms having small $\lambda$ values. Contrastingly, the present $|\Delta g_\perp|$ values are smaller than those for $X^2\Sigma_{(u)}^+$ dihalogen anions with fifteen VEs (16 200, 24 000 and 34 400 ppm for $F_2^-$, $FCl^-$, and $Cl_2^-$),[11,12] whose SOMOs are of $p_\sigma$ character, and where the atomic $\lambda$ values are large ($-270$ to $-590$ cm$^{-1}$). The intermediate position taken by the nine VE $|\Delta g_\perp|$ values is in line with the small to medium $p_\sigma$ contributions from both M and X to the SOMO.

The *g* shifts calculated for classes I and II radicals reproduce the experimental results quite well. For class III systems, ESR spectra are available only for BO, BS, and AlO. For BO and BS, our $\Delta g_\perp(R_e)$ values are also in good agreement with the experimental data. For AlO, a calculated value of $-2280$ ppm lies in the observed range, but all measurements have been performed in matrixes, which usually add negative contributions to the shifts.[3,65]

Interestingly, spin-rotation coupling constants $\gamma$ for $^2\Sigma^+$ states, obtained from microwave or optical spectra, can be correlated to $\Delta g_\perp$ values via Curl's equation. Experimental $\gamma$ values have been reported for all neutral radicals of class III. Taking as reference the most accurate microwave data, for BO our result $\Delta g_\perp = -1900$ ppm is compared with $-1915$ ppm derived from $\gamma_0$, for BS we compare our $-8450$ ppm with $-9300$ ppm, for AlO we compare our $-2280$ with $-1450$ ppm, and for AlS we compare our $-6915$ with $-4315$ ppm. All $\Delta g_\perp$ values derived from $\gamma_0$ should be less negative than $\gamma_e$. So again, BO and BS look reasonable, but AlO and AlS are somewhat in error.

Focusing on the particular case of AlO, ESR results show that $\Delta g_\perp$ becomes more negative with higher inert gases. It is $-1900$, $-2600$, and $-5000$ ppm for Ne, Ar, and Kr, respectively. A new experiment in Ne gives $-1200$ ppm. On the other hand, gas-phase spin-rotation constants (at $v = 0$) lead to about $-1450$ ppm on average. Since the matrix usually adds negatively,[3] the latest Ne result seems to be too small. Extrapolating from microwave $\gamma_v$ values for $v = 0-2$ to $\gamma_e$, a value of $-1800$ to $-1900$ ppm for $(\Delta g_\perp)_e$ is obtained, to be contrasted with our calculated value of $-2280$ ppm. As pointed out before, $\Delta g_\perp$ is particularly sensitive to the $\Delta E$ calculated for $1^2\Pi_i$, about 1 eV. An error of 0.1 eV, within the range accepted for these calculations, changes the $1^2\Pi_i$ contribution by about 10% (for example, $\Delta E = 0.9$ eV leads to $\Delta g_\perp(\text{tot}) \approx -2040$ ppm, close to the experimental gas-phase estimate).

In future studies, vibrational averaging is intended for $\Delta g_\perp$-(AlO),[66] to compare the theoretical results with $(\Delta g_\perp)_0$ in matrixes as well as with $(\Delta g_\perp)_v$ obtained from $\gamma_v$ data in the gas phase. Since $\Delta E(1^2\Pi_i)$ of AlO becomes smaller at larger bond distances, its positive contribution to $\Delta g_\perp$ therefore increases, and the overall negative value for $\Delta g_\perp$ will be reduced for increasing $v$. In fact, a change to positive $\Delta g_\perp$ values is expected at higher $v$ levels, as suggested by the equivalent change in the sign of $\gamma$ for $v = 2$. Obviously, similar large changes in the perpendicular *g* shifts with $v$ are expected for other radicals with a very low $\Delta E(1^2\Pi_i)$, such as $BN^-$, $BP^-$, $AlN^-$, and AlS.

For illustrative purposes, we have carried out model calculations on the $v$ dependency of $\Delta g_\perp$(AlO) *due to the coupling with* $1^2\Pi_i$ *alone*, to be reported in more detail elsewhere.[66] We took as input the SO($R$) and $L$ parameters, and RKR potentials, used by Ito et al.[45] in their analysis of the experimental $\gamma_v$ data. Our calculations give a $\Delta g_\perp(1^2\Pi_i)$ value of 1650 ppm at $R_e$, and of 2270 ppm for the vibrational average $v = 0$; i.e., the $1^2\Pi_i$ contribution to $(\Delta g_\perp)_{v=0}$ is larger than that at $R_e$, as said above. On the other hand, Ito et al.[45] found that $1^2\Pi_i$ contributes $-0.001\,88$ cm$^{-1}$ to $\gamma_0$, corresponding to $\Delta g'_\perp \approx 1600$ ppm, i.e., about 700 ppm smaller than the directly calculated $(\Delta g_\perp)_{v=0}$ value.

It would be of interest to record the ESR spectra of $AlN^-$ and $AlP^-$ to prove our predictions of positive $\Delta g_\perp$ values. To the best of our knowledge, these anions have not yet been synthesized in the laboratory. An MRCI study[27] carried out by us indicated that $AlP^-$ is very stable—about seven electronic states lie below neutral AlP—and therefore worthy of being studied experimentally.

Determination of the vibrational dependency of $\gamma$ for both $AlX^-$ anions would be desirable as well. Our $\Delta g_\perp$ calculations suggest that their spin-rotation constants should be *negative* for $v = 0$ (an anomalous sign when compared with other nine VE systems) but *positive* for low-lying $v$. Such a change in the sign of $\gamma$ is opposite that measured for AlO and AlS upon vibrational excitation.

**Acknowledgment.** We thank the NSERC (Canada) for financial support, and Dr. G. H. Lushington for helpful comments.

## References and Notes

(1) Carrington, A.; McLachlan, A. D. *Introduction to Magnetic Resonance*; Harper and Row: New York, 1967.

(2) Harriman, J. E. *Theoretical Foundations of Electron Spin Resonance;* Academic Press: New York, 1978.

(3) Weltner, W. *Magnetic Atoms and Molecules*; Dover: New York, 1983.

(4) Bruna, P. J.; Lushington. G. H.; Grein, F. *Chem. Phys. Lett.* **1996**, *258*, 427.

(5) Lushington, G. H.; Bruna, P. J.; Grein, F. *Int. J. Quantum Chem.* **1997**, *63*, 511.

(6) Bruna, P. J.; Lushington, G. H.; Grein, F. To be published.

(7) Lushington, G. H.; Grein, F. *J. Chem. Phys.* **1997**, *106*, 3292.

(8) Lushington, G. H.; Grein, F. *Int. J. Quantum Chem.* **1996**, *60*, 1679.

(9) Bruna, P. J.; Grein, *Int. J. Quantum Chem.* **2000**, *76*, 447.

(10) Bruna, P. J.; Grein, F. *J. Chem. Phys.* **2000**, *112*, 10796.

(11) Bruna, P. J.; Grein, F. *Chem. Phys.* **1999**, *249*, 169.

(12) Bruna, P. J.; Grein, F. *Chem. Phys. Lett.* **2000**, *318*, 263.

(13) Huber, K. P.; Herzberg, G. *Molecular Spectra and Molecular Structure, IV. Constants of Diatomic Molecules*; Van Nostrand: New York, 1979.
(14) Bruna, P. J.; Grein, F. *J. Phys. Chem.* **1992**, *96*, 6617.
(15) Bruna, P. J.; Dohmann, H.; Peyerimhoff, S. D. *Can. J. Phys.* **1984**, *62*, 1508.
(16) Bruna, P. J.; Peyerimhoff, S. D. *Adv. Chem. Phys.* **1987**, *67*, 1.
(17) Bruna, P. J.; Dohmann, H.; Anglada, J.; Krumbach, V.; Peyerimhoff, S. D.; Buenker, R. J. *J. Mol. Struct.: THEOCHEM* **1983**, *93*, 309. Bruna, P. J.; Peyerimhoff, S. D. *Bull. Soc. Chem. Belg.* **1983**, *92*, 525. Arnold, C. C.; Kitsopoulos, T. N.; Neumark, D. M. *J. Chem. Phys.* **1993**, *99*, 766.
(18) Davies, D. W. *The Theory of the Electric and Magnetic Properties of Molecules*; John Wiley: London, 1967.
(19) Bruna, P. J.; Grein, F. To be published.
(20) Bruna, P. J.; Grein, *Int. J. Quantum Chem.* **2000**, *77*, 324.
(21) (a) Clark, T.; Chandrasekhar, J.; Spitznagel, G. W.; Schleyer, P. v. R. *J. Comput. Chem.* **1983**, *4*, 294. Frisch, M. J.; Pople, J. A.; Binkley, J. S. *J. Chem. Phys.* **1984**, *80*, 3265. (b) McLean, A. D.; Chandler, G. S. *J. Chem. Phys.* **1980**, *72*, 5639.
(22) Frisch, M. J.; Head-Gordon, M.; Trucks, G. W.; Foresman, J. B.; Schlegel, H. B.; Raghavachari, H.; Robb, M. A.; Binkley, J. S.; Gonzalez, C.; DeFrees, D. F.; Fox, D. F.; Whiteside, R. A.; Seeger, R.; Melius, C. F.; Baker, J.; Martin, R. L.; Kahn, L. R.; Stewart, J. P.; Topiol, S.; Pople, J. A. GAUSSIAN90, Gaussian Inc., Pittsburgh, 1990.
(23) Lushington, G. H. Ph.D. Thesis, University of New Brunswick, Fredericton, New Brunswick, Canada, 1996.
(24) Lushington, G. H.; Bündgen, P.; Grein, F. *Int. J. Quantum Chem.* **1995**, *55*, 377. Bündgen, P.; Lushington, G. H.; Grein, F. *Int. J. Quantum Chem., Symp.* **1995**, *29*, 283. Lushington, G. H.; Grein, F. *Theor. Chim. Acta* **1996**, *93*, 259.
(25) Buenker, R. J.; Peyerimhoff, S. D. *Theor. Chim. Acta* **1974**, *35*, 33; **1975**, *39*, 217. Buenker, R. J.; Peyerimhoff, S. D.; Butscher, W. *Mol. Phys.* **1978**, *35*, 771. Buenker, R. J. In *Studies in Physical and Theoretical Chemistry. Current Aspects of Quantum Chemistry*; Carbó, R., Ed.; Elsevier: Amsterdam, 1982; Vol. 21, p 17. Marian, C. Ph.D. Thesis, Bonn, Germany, 1981. Hess, B. A. Ph.D. Thesis, Bonn, Germany, 1981. Chandra, P.; Buenker, R. J. *J. Chem. Phys.* **1983**, *79*, 358, 366.
(26) Mawhinney, R. B.; Bruna, P. J.; Grein, F. *Can. J. Chem.* **1993**, *71*, 1581. Bruna, P. J.; Mawhinney, R. B.; Grein, F. *Int. J. Quantum Chem., Symp.* **1995**, *29*, 455.
(27) Bruna, P. J.; Grein, F. *J. Phys. B: At. Mol. Opt. Phys.* **1989**, *22*, 1913.
(28) Luzanov, A. V.; Babich, E. N.; Ivanov, V. V. *J. Mol. Struct.: THEOCHEM* **1994**, *331*, 211.
(29) Baeck, K. K.; Bartlett, R. J. *J. Chem. Phys.* **1997**, *106*, 4604.
(30) Glenewinkel-Meyer, T.; Müller, B.; Ottinger, C.; Rosmus, P.; Knowles, P. J.; Werner, H.-J. *J. Chem. Phys.* **1991**, *95*, 5133. Knowles, P. J.; Werner, H.-J. *Theor. Chim. Acta* **1992**, *84*, 95.
(31) Sennesal, J. M.; Robbe, J. M.; Schamps, J. *Chem. Phys.* **1981**, *55*, 49.
(32) Dyke, J. M.; Kirby, C.; Morris, A.; Gravenor, B. W. J.; Klein, R.; Rosmus, P. *Chem. Phys.* **1984**, *88*, 289.
(33) Glenewinkel-Meyer, T.; Kowalski, A.; Müller, B.; Ottinger, C.; Breckenridge, W. H. *J. Chem. Phys.* **1988**, *89*, 7112.
(34) Marian, C. M. *Chem. Phys.* **1985**, *100*, 13.
(35) Lushington, G. H.; Bruna, P. J.; Grein, F. *Z. Phys. D* **1996**, *36*, 301. Bruna, P. J.; Lushington, G. H.; Grein, F. *Chem. Phys.* **1997**, *225*, 1. Bruna, P. J.; Grein, F. *J. Chem. Phys.* **1998**, *109*, 9439. Bruna, P. J.; Grein, F. *J. Phys. Chem. A* **1998**, *102*, 3141. Bruna, P. J.; Grein, F. *J. Phys. Chem. A* **1999**, *103*, 3294.
(36) Richards, W. G.; Trivedi, H. P.; Cooper, D. L. *Spin−orbit Coupling in Molecules*; Clarendon Press: Oxford, 1981.
(37) Lefebvre-Brion, H.; Field, R. W. *Perturbation in the Spectra of Diatomic Molecules*; Academic Press: Orlando, 1986.
(38) Knight, L. B.; Wise, M. B.; Childers, A. G.; Davidson, E. R.; Daasch, W. R. *J. Chem. Phys.* **1980**, *73*, 4198.
(39) Buckingham, A. D.; Olegário, R. M. *Chem. Phys. Lett.* **1993**, *212*, 253.
(40) (a) Ohshima, Y.; Endo, Y. *Chem. Phys. Lett.* **1993**, *213*, 95. (b) Anderson, M. A.; Ziurys, L. M. *Chem. Phys. Lett.* **1994**, *224*, 381.
(41) Gutsev, G. L.; Nooijen, M.; Bartlett, R. J. *Chem. Phys. Lett.* **1997**, *276*, 13.
(42) Cooper, D. L.; Prosser, S. J.; Richards, W. G. *J. Phys. B: At. Mol. Phys.* **1981**, *14*, L487.
(43) Brom, J. M.; Weltner, W. *J. Chem. Phys.* **1972**, *57*, 3379.
(44) Mahieu, J. M.; Jacquinot, D.; Schamps, J.; Hall, J. A. *J. Phys. B: At. Mol. Phys.* **1975**, *8*, 308.
(45) Ito, H. *Can. J. Phys.* **1994**, *72*, 1082. Goto, M.; Takano, S.; Yamamoto, S.; Ito. H.; Saito, S. *Chem. Phys. Lett.* **1994**, *227*, 287. Ito, H.; Goto, M. *Chem. Phys. Lett.* **1994**, *227*, 293.
(46) Coxon, J. A.; Foster, S. C.; Naxakis, S. *J. Mol. Spectrosc.* **1984**, *105*, 465.
(47) Schamps, J. *Chem. Phys.* **1973**, *2*, 352. Yoshimine, M.; McLean, A. D.; Liu, B. *J. Chem. Phys.* **1973**, *58*, 4412. Lengsfield, B. H.; Liu, B. *J. Chem. Phys.* **1982**, *77*, 6083. Zenouda, C.; Blottiau, P.; Chambaud, G.; Rosmus, P. *J. Mol. Struct.: THEOCHEM* **1999**, *458*, 61.
(48) Karna, S. P.; Grein, F. *J. Mol. Spectrosc.* **1987**, *122*, 356.
(49) Martinez de Pinillos, J. V.; Weltner, W. J. *J. Chem. Phys.* **1976**, *65*, 4256.
(50) Schreckenbach, G.; Ziegler, T. *J. Phys. Chem. A* **1997**, *101*, 3388; *Theor. Chim. Acc.* **1998**, *99*, 71.
(51) (a) Jayatilaka, D. *J. Chem. Phys.* **1998**, *108*, 7587. (b) Lushington, G. H. *J. Phys. Chem. A* **2000**, *104*, 2969.
(52) Knight, L. B.; Wise, M. B.; Childers, A. G.; Daasch, W. R.; Davidson, E. R. *J. Chem. Phys.* **1981**, *74*, 4256.
(53) Knight, L. B.; Easley, W. C.; Weltner, W.; Wilson, M. *J. Chem. Phys.* **1971**, *54*, 322.
(54) Knight, L. B.; Ligon, A.; Cobranchi, S. T.; Cobranchi, D. P.; Earl, E.; Feller, D.; Davidson, E. R. *J. Chem. Phys.* **1986**, *85*, 5437.
(55) Knight, L. B.; Earl, E.; Ligon, A.; Cobranchi, D. P.; Woodward, J. R.; Bostick, J. M.; Davidson, E. R.; Feller, D. *J. Am. Chem. Soc.* **1986**, *108*, 5065.
(56) (a) Knight, L. B.; Easley, W. C.; Weltner, W. *J. Chem. Phys.* **1971**, *54*, 1610. Knight, L. B.; Wise, M. B.; Davidson, E. R.; McMurchie, L. E. *J. Chem. Phys.* **1982**, *76*, 126. (b) Knight, L. B.; Herlong, J. O.; Kirk, T. J.; Arrington, C. A. *J. Chem. Phys.* **1992**, *96*, 5604.
(57) (a) Knight, L. B.; Weltner, W. *J. Chem. Phys.* **1971**, *55*, 5066. Knight, L. B.; Ligon, A.; Davidson, E. R.; McMurchie, L. E. *J. Chem. Phys.* **1982**, *76*, 126. (b) Knight, L. B.; Kirk, T. J.; Herlong, J.; Kaup, J. G.; Davidson, E. R. *J. Chem. Phys.* **1987**, *107*, 7011.
(58) Curl, R. F. *Mol. Phys.* **1965**, *9*, 585. Knight, L. B.; Weltner, W. J. *J. Chem. Phys.* **1970**, *53*, 4111.
(59) Takano, S.; Yamamoto, S.; Saito, S. *J. Chem. Phys.* **1990**, *94*, 3355.
(60) Launila, O.; Jonsson, J. *J. Mol. Spectrosc.* **1994**, *168*, 483.
(61) (a) Törring, T.; Herrmann, R. *Mol. Phys.* **1989**, *68*, 1379. (b) Yamada, C.; Cohen, E. A.; Fujitake, M.; Hirota, E. *J. Chem. Phys.* **1990**, *92*, 2146.
(62) Launila, O.; Jonsson, J. *J. Mol. Spectrosc.* **1994**, *168*, 1.
(63) Bruna, P. J.; Lushington, G. H.; Grein, F. *J. Mol. Struct.: THEOCHEM* **2000**, *527*, 139.
(64) Bader, R. F. M.; Beddall, P. M.; Cade, P. E. *J. Am. Chem. Soc.* **1971**, *93*, 3095.
(65) Knight. L. B.; Steadman, J. *J. Chem. Phys.* **1984**, *80*, 1018.
(66) Unpublished results from this laboratory.
(67) Parlant, G.; Rostas, J.; Taieb, G.; Yarkony, D. R. *J. Chem. Phys.* **1990**, *93*, 6403.
(68) Dyke, J. M.; Kirby, C.; Morris, A. *J. Chem. Soc., Faraday Trans. 2* **1983**, *79*, 483. Rosmus, P.; Werner, H.-J.; Grimm, M. *Chem. Phys. Lett.* **1982**, *92*, 250.
(69) Tanimoto, M.; Saito, S.; Hirota, E. *J. Chem. Phys.* **1986**, *84*, 1210.
(70) Mélen, F.; Dubois, I.; Bredohl, H. *J. Phys. B: At. Mol. Phys.* **1985**, *18*, 2423.
(71) Dunn, T. M.; Hanson, L. *Can. J. Phys.* **1969**, *47*, 1657.
(72) Tanimoto, M.; Saito, S.; Yamamoto, S. *J. Chem. Phys.* **1988**, *88*, 2296.
(73) (a) Zeeman, P. B. *Can. J. Phys.* **1951**, *29*, 336. (b) Jenouvrier, A.; Pascat, B. *Can. J. Phys.* **1981**, *59*, 1851.
(74) Lavendy, H.; Mahieu, J. M.; Becart, M. *Can. J. Spectrosc.* **1973**, *18*, 13.